The Surface Properties of Teeth Treated with Resin Infiltration or Amorphous Calcium Phosphate

A THESIS

Presented to the Faculty of

The Air Force Postgraduate Dental School

Of the Uniformed Services University

Of the Health Sciences

In Partial Fulfillment

Of the Requirements

For the Degree of
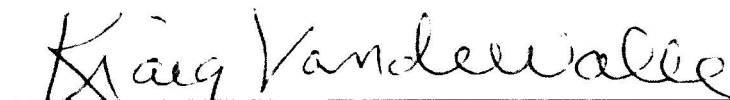
MASTER OF SCIENCE

In Oral Biology

By

Todd Andrew Lincoln, BA, DDS

Dunn Dental Clinic
Lackland AFB, TX
4 May 2012

The Surface Properties of Teeth Treated with Resin Infiltration or Amorphous Calcium Phosphate
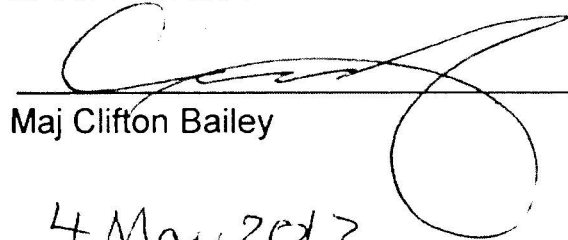
Todd Andrew Lincoln

APPROVED:

Kraig Vandewalle
Col Kraig Vandewalle

[signature]
Lt Col Wen Lien

[signature]
Maj Clifton Bailey

4 May 2012
Date

APPROVED:

[signature]
Col Thomas R. Schneid
Dean, Air Force Postgraduate Dental School

DEDICATION

I am honored and blessed to be married to a fellow USAF dentist, Major (Dr) Ketu P. Lincoln. It is her inspiration and words of encouragement that have carried me through this project and to her I owe the determination to continue to stretch for an invisible finish line. Now it's my turn to give back what I have received from you these last 2 years so enjoy the pros residency. You will succeed where I have stumbled. Love you Baby!

My 2 daughters, Lily and Nyah are everything a father could wish for and more. They see this old guy doing what it takes night after night and hopefully I have been an inspiration to them. Their shining faces and silliness have kept a smile on my face throughout this research project and especially when a smile was hard to find. Always remember success is in the journey and not the result. Love you girls!

In loving memory of my parents Irving and Libby. Dad always said, "Nobody can take that sheepskin away from you so stay in school." After 50 years dad, I am good. Mom, all of those late nights typing papers hours before they were due finally paid off. I can still hear your voice yelling at me for waiting until the last minute. I wish you both could know how much those memories mean today!

Last but not least, Ums, Bhavik and Bah thanks for all of the prayers and hope you gave me when it seemed there was none to be found. You are my extended family and you all are effortless in bringing hope to gloom. Thank you does not begin to explain how much everything you do for me truly means. Love you guys!

ACKNOWLEDGEMENTS

ABSTRACT

Objective: This study compared the properties of color stability and surface roughness of demineralized enamel treated with resin infiltration (ICON) or with casein phosphopeptide-amorphous calcium phosphate (MI Paste, CPP-ACP). **Methods**: Fifty human enamel blocks (4 x 4 mm^2) were prepared. Each block was treated with 1M HCl (pH 1.5) solution for 2 minutes to create an accelerated surface mineral loss and randomly assigned into five groups (n = 10): Group 1 (Control) was untreated and stored in saliva, Group 2 was treated with ICON per manufacturer instructions and stored in saliva, Group 3 was treated with CPP-ACP for 3-5 minutes daily for one month and stored in saliva, Group 4 was treated with ICON per manufacturer instructions and stored in water, Group 5 was treated with CPP-ACP for 3-5 minutes daily for one month and stored in 100% humidity. Specimens immersed in saliva were stored at 37°C. The facial surface profilometry of each block was measured at baseline and immediately after surface mineral loss, immediately after surface treatment, and at days 3 and 30 using a non-contact profilometer (Proscan-2000, Scantron, UK). The assessment of color was performed by a spectrophotometer (VITA Easyshade® Compact, Vident, Brea, CA, USA). For all groups, color measurements were made at baseline for each group, immediately after surface mineral loss and at days 3 and 30. Each of the surface measurements was performed three times, and a mean calculated. The means and

standard deviations of surface roughness (Ra), surface waviness (Sm), changes in luminance (Delta L*), and changes in Sm (Delta Sm) were analyzed by one-way analysis of variance (ANOVA, alpha = 0.05), and the Tukey-Kramer multiple comparison procedure was used for post hoc comparisons. **Results:** Significant differences were seen in Delta L*, Sm, and Delta Sm (see Figures 1, 3, and 4 respectively). Significant changes were observed in surface roughness for the Group-4 (ICON-Water), but surface treatments did not provide the expected results of returning the Ra values to baseline values for Group 2, 3, and 5 (see Figure 2).

Conclusion: The results of this study do not provide conclusive evidence that the standard of care for enamel demineralization and potential remineralization should shift towards the application of ICON or MI Paste^{TM} / Plus^{TM} technologies.

TABLE OF CONTENTS

LIST OF TABLES

LIST OF FIGURES

I.   BACKGROUND AND LITERATURE REVIEW

A.   Caries

Epidemiology

Today, dental caries remains one of the most common chronic diseases throughout the world. If left untreated, caries can lead to pain and infection causing dental emergencies that can significantly affect an individual's quality of life. According to a recent national survey, approximately 16% of children, ages 6-19 years, and 23% of adults, ages 20-64 years, have untreated dental caries (Health, United States: 2010, Table 93). Even though Americans of all ages have been gradually improving their oral health over the past decade, dental caries continues to be the most prevalent oral disease in several Asian and Latin American countries (Petersen et al 2005). Great strides have been made to describe the underlying etiology of dental caries. However, there is still much that is unknown. Thus, a necessary first step in preventing dental caries is to understand its multifaceted nature.

Definition and Biofilm-Dependent Process

Dental caries is a biofilm-dependent oral disease, and its commencement relies on the complex interactions between different species of aerobic and anaerobic microorganisms and the host. Under the right circumstances oral microbes have the ability to colonize by adhering to teeth. They produce copious amounts of acidic

1

byproducts to evade the host immune system and continue to thrive in a low pH environment. The specific pathogenic species of dental caries are streptococcus mutans and lactobacilli acidophilus. These bacteria produce lactic, acetic, formic and propionic acids, which have been shown to readily dissolve enamel and dentinal tissues (Featherstone et al 1981, 2000). The current theory suggests that the caries process is initiated in the presence of a cariogenic biofilm or dental plaque (Fejerskov et al 1990, Manji et al 1991, Fejerskov et al 1994). Shortly after tooth eruption or cleansing, surfaces of teeth become coated with an acellular organic film. This conditioned film or pellicle is formed mainly from salivary glycoproteins, proteins, food, gingival crevicular fluid, or blood. Biofilm initiates with the attachment of planktonic microorganisms to the surface of the pellicle via weak, long-range physicochemical forces (Wimpenny 1994). These pioneer species multiply and produce an extracellular polymeric matrix, which acts as a reservoir for diffusing molecules, enzymes, and proteins and allows the emerging biofilm community to develop into a complex, three-dimensional structure. The bacteria within the biofilm respond collectively through quorum sensing and express factors leading to the maturation of a polysaccharide matrix (Hojo et al 2009). When frequent sucrose consumption becomes a routine diet, the fermentable carbohydrates induce a lower overall oral pH (5.5 or below) and trigger a shift in the balance of resident plaque microflora to a more cariogenic state (Stephan 1944). Thus, this acidic biofilm is responsible for the biochemical and physiological changes in dental hard tissues.

White Spot Lesions

Most dental caries begin with formation of a white spot lesion. White spot or incipient (noncavitated) lesions represent an imbalance of mineral exchanges between the tooth and the surrounding environment creating an osmotic gradient which drives undersaturation and supersaturation conditions with respect to the enamel hydroxyapatite crystals. Although enamel crystals under normal physiology regularly go through natural periods of demineralization and remineralization, undersaturation occurs mainly under acidic conditions created by the resident cariogenic microflora as explained earlier. For example, the hydrogen ions, which are produced by the metabolic activity of the covering biofilms in the presence of fermentable carbohydrates, dissolve calcium and phosphate into the surrounding aqueous phase (LeGeros 1991, Nelson 1982, 1983, 1984). After a period of time and with normal salivary flow, minerals are released from saliva, biofilm, and the tooth surface itself in response to the differential osmotic gradient resulting in a supersaturation condition (LeGeros et al 1968, 1991). During this period of supersaturation minerals can remineralize partially demineralized enamel crystals and is the body's natural process for repairing noncavitated incipient lesions (LeGeros 1991, Nelson et al 1982, 1983, 1984). It is important to realize that pH is a strong determinant for balancing the osmotic gradient, but other factors such as the concentration of calcium and phosphate ions, the total ionic strength of the plaque fluid, and fluxes of enzymes and proteins play an equally key role in mitigating the process of demineralization and remineralization (Margolis et al., 1994). White spot

lesions are clinical signs portraying incipient caries in the stage of initiation or being arrested. Their surface coloration is a response to light scattering in response to varying degrees of demineralization and remineralization. Most chalky surfaces of a white spot lesion characterize significant loss of translucency as a result of acids diffusing through the demineralized enamel from the overlaying biofilms (Featherstone 1999, 2000, 2004). Cycles of demineralization and remineralization continue in the mouth as long as there are cariogenic bacteria, fermentable carbohydrates and saliva present.

B.   Minimally Invasive Dentistry

Clinical decision-making for caries management depends on the multiplicity of factors that influence dental caries. Besides diagnostic acumen, recognizing risk factors like past and current caries experience, oral microbial prevalence, salivary status, medical history, and one or more social, behavioral, and demographic characteristics are keys to planning successful preventive strategies and appropriate treatment modalities. For decades, the treatment philosophy behind restorative dentistry has remained largely unchanged. However, echoing similar trends in medicine there is increasing interest in minimal tissue removal, risk assessment, and early detection and prevention. As advances in dental research continue and our growing understanding of the caries process grows there is a revolutionary urge for material novelties and for a shift in the treatment paradigm. G. V. Black's teachings

of extension for prevention have given way to the present day mantra of minimum intervention. Minimally invasive dentistry is defined as "a systematic respect for the original tissue" (White et al 2000, Ericson et al 2003). The intention of this approach is to base patient treatments on a combined use of clinical expertise, technical competence, and current best regenerative-medicine evidence.

In clinical practice the ultimate goal of caries management by operative dentistry is to restore dental health including the restoration of form, function, phonetics, esthetics, and occlusal stability. Despite the success of the traditional surgical model for treating cavitated lesions, the medical model extends the longevity of noncavitated carious teeth. The tenets of this philosophy are to preserve intact tooth structure reducing trauma to the pulp tissue, and to decrease risk for future recurrent caries by promoting oral wellness (White et al 2000, Ericson et al 2003). The medical model focuses on methods to arrest or reverse the non-cavitated lesion and on eliminating the bacterial risk factors through counseling on dietary practices, tooth brushing, and topical application of antibacterial agents. The most commonly used topical agent for battling dental caries is fluoride. Other commonly used chemotherapeutic agents include chlorhexidine, povidine iodine, and tricolsan (Matthijs S et al 2002, Du MQ et al 2008, Milgrom P et al 2009, Ly KA et al 2008, Berkowitz RJ et al 2009, Lopez L et al 2002, Lopez L et al 2009, Yee R et al 2009).

The ability of fluoride to inhibit and reverse the initiation and progression of dental caries is well documented (Curry et al 2004, Ellwood et al 2008, Fejerskov et al 1996). As cariogenic bacteria metabolize carbohydrates and produce acid, the presence of fluoride ions enhances remineralization by making the tooth surface less soluble (Casals et al 2007, Curry et al 2004, Fejerskov et al 1996, ten Cate 1999). Consequently, the fluoride ions attract calcium and phosphate ions and further drive the partially demineralized crystal surface to a new supersaturated state. The partially dissolved enamel crystals interact with fluoride ions which enable remineralization. When the enamel surface crystal composition is chemically integrated with fluoride, hydroxyapatite fluorapatite reduces the critical pH for mineral dissolution during demineralization.

Minimal intervention is a key phrase in today's dental practice. Minimal intervention dentistry (MID) focuses on the least invasive treatment possible as a means of minimizing tissue loss and patient discomfort. Concentrating mainly on prevention and early intervention of caries, MID's first basic principle is the remineralization of early carious lesions, advocating a biological or therapeutic approach rather than the traditional surgical approach for early surface lesions. One of the key elements of a biological approach is the usage and application of remineralizing agents to tooth structure (enamel and dentin lesions). These agents are part of a new era in dentistry aimed at controlling the demineralization/ remineralization cycle depending upon the microenvironment of the tooth. The remineralizing properties of saliva can

be enhanced using materials which release biologically available calcium, phosphate and fluoride ions (Rao et al 2011).

C. Casein Phosphopeptide – Amorphous Calcium Phosphate (CPP-ACP)

In the oral environment, tooth structure undergoes continuous demineralization and remineralization (Featherstone et al 2004). If this balance is disrupted, demineralization will progress leading to a deterioration of the tooth structure. Milk and milk-related products such as cheese have been shown to have anticariogenic properties in human and animal models (Reynolds et al 1981, Rosen et al 1984). According to past research, the mechanism of this action is due to a direct chemical effect from phosphoprotein casein and calcium phosphate components of the cheese (Krobicka et al 1987, Harper et al 1986). Casein phosphopeptides (CPP) have the ability to stabilize calcium phosphate in solution through binding amorphous calcium phosphate (ACP) with their multiple phosphoserine residues. This allows the formation of small CPP–ACP clusters. These CPP-ACP clusters act as a calcium and phosphate reservoir that binds to dental plaque and tooth surfaces. Upon acid challenge, the attached CPP-ACP releases calcium and phosphate ions maintaining a supersaturated mineral environment thereby reducing demineralization and enhancing remineralization (Reynolds et al 2003, Manton et al

2008). It has been shown that enamel remineralized by CPP-ACP is relatively more acid-resistant than normal tooth enamel (Cai et al 2007, Iijima et al 2004).

Calcium and phosphate ions have been proposed as necessary adjuncts in the remineralization process to supplement the use of fluoride (Reynolds 2009). Found in saliva, calcium and phosphate are the building blocks of remineralization. The variability between individuals with respect to salivary glands and secretion rates means that the degree of saturation of these ions is not equal per individual. The dissolution and precipitation of tooth minerals depends on the pH and the concentration of ions in the fluid phase surrounding the tooth structures (ten Cate 2004).

Calcium phosphate remineralization technology has now been developed based on casein phosphopeptide-amorphous calcium phosphate (CPP-ACP) [RecaldentTM CASRN691364-49-5], where it is claimed that the CPP stabilizes high concentrations of calcium and phosphate ions together with fluoride ions at the tooth surface by binding to pellicle and plaque. Although the calcium, phosphate, and fluoride ions are stabilized by the CPP from promoting dental calculus, the ions are freely bioavailable to diffuse down concentration gradients into enamel subsurface lesions, thereby effectively promoting remineralization *in vivo* (Reynolds 2009). CPP containing the active sequence –Ser(P)-Ser(P)-Ser(P)-Glu-Glu- has a remarkable ability to stabilize calcium and phosphate as nanoclusters of ions in a metastable

solution (Cochrane, 2008). Through the active sequence, CPP binds to forming nanoclusters of calcium and phosphate ions to form nanocomplexes of about a 1.5 nm radius, preventing the growth of the nanoclusters to the critical size required for nucleation and phase transformation. This prevents the crystals from growing to critical size and precipitating out of solution (Reynolds 1998). The remineralization process is enhanced by the biologically active amorphous calcium phosphate, which is able to release calcium and phosphate. It has been shown in vitro that CPP-ACP was effective in the remineralization of carious lesions (Reynolds 1997, Featherstone et al 2007, Hicks et al 2006). The disadvantage to CPP-ACP is the need for repeated applications.

D.   ICON

Recently, a new "infiltration" approach to target incipient caries has been introduced. According to the manufacturer, caries infiltration (ICON) has been proposed as a means to arrest intermediary lesions in one visit with no mechanical preparation or anesthesia. The penetration and arrest of artificial lesions by dental adhesives and fissure sealants has been investigated in several laboratory studies (Rodda 1983, Donly et al 1992, Robinson et al 2001, Gray et al 2002, Schmidlin et al 2004, Meyer-Lueckel et al 2008; Paris et al, 2006). However, dental sealants and adhesives are not optimized for high penetrability and therefore only showed superficial penetration into natural enamel lesions

(Paris et al 2007). Special resins, optimized for rapid capillary penetration, so-called infiltrants, penetrate significantly deeper (Meyer-Lueckel et al 2008). The highest penetration coefficients have been found for mixtures containing tetraethyleneglycol dimethacrylate (TEGDMA), 2-hydroxyethyl methacrylate (HEMA) and 20% ethanol (Meyer-Lueckel et al 2008). Infiltrant has been shown to have a high penetration coefficient enabling it to be drawn deep within the pores of a lesion. Filling the lesion will reportedly arrest the caries progression (Kugel et al 2009). It has been proposed that the theory of tooth surfaces being intact adjacent to carious lesions, especially interproximal lesions, is false and that these surfaces are, in fact, not intact (Kielbasa et al 2006). Therefore, it is necessary to penetrate these "pseudo-intact" surface layers to reach the areas that the infiltrant can effectively wall off. With the infiltration technique, a diffusion barrier is formed in the inner parts of the lesion and the affected surface is restored with resin material. Commonly used in this technique is 15% HCl. Etching with phosphoric acid affected only the outermost 25 µm of the surface (Paris et al 2007). However, superficial phosphoric acid etching causes the caries lesion to extend into the deeper enamel layers. Consequently, cavitation may occur in the future. The penetration depth of 15% HCl etching is more than twice (58 µm) that of phosphoric acid, enabling penetration into the deepest part of the lesion and eliminating the decalcified areas, preventing further attacks (Meyer-Lueckel 2007). A rubber dam is necessary with all applications, because 15% HCl produces soft tissue ulceration within 30 seconds (Croll et al 1990).

Several studies have reported that 120 seconds is the optimum etching time (Paris et al 2010, Croll et al 1986). The primers and resin materials used contain solvents, such as ethanol, which increase the surface tension of enamel, enabling rapid penetration of resins into the lesions, increasing the adhesion strength (Meyer-Lueckel et al 2006, Martignon et al 2006).

II. OBJECTIVES

A. Objective Overview

The purpose of this study is to compare the remineralization of artificial white spot lesions with MI paste by GC to the infiltration of the lesions with ICON by DMG. Both products are marketed to target incipient caries by reducing the opaqueness of white spot lesions. Although numerous options such as fluoride application, sealants, chlorhexidine rinse, or xylitol usage exist for early caries progression, treating the lesions with ICON reportedly offers a technique of stopping the diffusion of bacteria and restoring the natural tooth shade without drilling or sacrificing healthy tooth structure (Ardu et al 2007). This study is primarily focused on the variables of color stability and surface morphology. By evaluating surface parameters like roughness, waviness, change in color between light and dark which will be known as change in luminance (Delta L*), and change in peak spacing average which will be known as change in surface waviness (Delta Sm), this study will quantitatively examine how resin infiltrant or MI paste can stabilize incipient lesions on teeth with accelerated surface mineral loss. The results should provide basic information to clinicians who use MI paste or ICON as to whether or not these novel materials can arrest incipient lesions and are indicated as options for treating early lesions. The outcome of this study may also clarify whether or not caries infiltration can effectively

mask demineralization and blend the treated lesions to their surrounding natural enamel.

B.   Specific Hypotheses

This study tested two specific null hypotheses as follows:

1)   There is no significant difference in color stability of enamel blocks whose surfaces are modified to simulate accelerated mineral loss when treated with resin infiltration or MI paste.

2)   There is no significant difference in surface morphology of enamel blocks whose surfaces are modified to simulate accelerated mineral loss when treated with resin infiltration or MI paste.

This study tested four alternative hypotheses as follows:

1)   ICON has a greater ability to restore the color of an enamel block with accelerated mineral loss to its original color than MI paste.

2)   ICON has greater ability to restore the surface morphology of an enamel block with accelerated mineral loss to its original surface morphology than MI paste.

3)   MI paste has greater ability to restore the color of an enamel block with accelerated mineral loss to its original color than ICON.

4)   MI paste has greater ability to restore the surface morphology of an enamel block with accelerated mineral loss to its original surface morphology than ICON.

13

III. MATERIALS AND METHODS

A. Experimental Design Overview

The materials used in this experiment were ICON by DMG America and MIP paste by GC Corporation (see Table 1).

A total of five groups were created (see Table 2). Ten enamel blocks (~ 4 mm x 4 mm) were prepared per group resulting in 50 total specimens. Each block was treated with 1M HCl (pH 1.5) solution for 2 minutes to create an accelerated surface mineral loss and randomly assigned into the five groups (n = 10): Group 1 (Control) was untreated and stored in saliva, Group 2 was treated with ICON per manufacturer instructions and stored in saliva, Group 3 was treated with MI paste for 3-5 minutes daily for one month and stored in saliva, Group 4 was treated with ICON per manufacturer instructions and stored in water, Group 5 was treated with MI paste for 3-5 minutes daily for one month and stored in 100% humidity. The baseline of color and surface profilometry of each block pre and post treatment were collected.

B.   Experimental Design

Enamel Block Preparation:

Twenty-five extracted human third molars were stored in 0.5% chloramine T and used within 6 months following extraction. The facial and lingual surfaces were sectioned with a diamond disc to prepare fifty enamel blocks (~ 4 mm x 4 mm). Ten enamel blocks were randomly assigned to each group. The enamel blocks were polished using fine pumice to remove adherent pellicle which could form a barrier to acid attack then brushed under running water and allowed to dry. The blocks were immersed for 2 minutes in 1M hydrochloric acid solution at 25ºC to create an accelerated surface mineral loss. After lesion formation, all the specimens were rinsed with distilled water and immediately used for different surface treatments.

ICON and MI paste Treatments:

Please refer to table 1 for details of the materials used and table 2 for the study groups and the treatments administered for each group. Enamel blocks in Group 1 served as control and receive no surface treatment after accelerated surface mineral loss. Specimens in Group 2 and Group 4 were restored with ICON according to the manufacturer's instructions. The main difference in these groups is that Group 2 is stored in artificial saliva then placed in a lab oven (#20GC, H&C Thermal Systems, Columbia, MD) at 37°C and Group 4 is stored in distilled water at 37°C. The storage medium for both groups was changed daily and each group was kept in the lab oven

15

for the duration of the consecutive 30 day period. For ICON application, the smooth surface tip was applied to the ICON-etch syringe, and the etchant was applied and allowed to set for 2 minutes. The etchant was rinsed for 30 seconds. The application cannula was screwed onto the Icon-dry syringe, half the syringe was applied and allowed to stand for 30 seconds before drying with an air-water syringe. A smooth-surface tip was screwed onto the ICON-infiltrate syringe. The infiltrant was applied and allowed to set for 3 minutes. The excess material was removed with a cotton roll and was light cured for 40 seconds. A new smooth-surface tip was screwed onto the syringe, and the infiltrant was applied a second time using the same sequence of steps and was allowed to set for 1 minute and light cured for 40 seconds.

For specimens in Group 3 and Group 5, 0.05 mL of MI paste was injected onto the surface of the enamel using a 1-mL syringe (Luer-Lok, BD, Franklin Lakes, NJ) with a 20-gauge needle. A micro-brush was used to evenly paint the MI paste over the top facial surface of each enamel block.   For Group 3, the specimens painted with MI paste were placed in a lab oven at 37°C and 95±5% relative humidity for 5 minutes. After five minutes, the specimens were placed into artificial saliva in the lab oven. After 30 minutes of submersion, the MI Paste was rinsed off using 30ml of distilled water for 15 seconds. The specimens were placed back into the lab oven in artificial saliva. The artificial saliva was changed daily. The procedure was repeated daily for 30 consecutive days. The enamel specimens were kept in the lab oven

16

throughout the duration of the experiment and were removed only for MI paste application and rinsing procedures.

For Group 5, the specimens painted with MI paste were placed in the lab oven at 37°C and 95±5% relative humidity for 5 minutes. After 30 minutes, the MI paste was rinsed off using 30ml of distilled water for 15 seconds. The specimens were placed back into the lab oven at 37°C and 95±5% relative humidity. It is important to note the difference here in comparison to Group 3 which was stored in a solution of artificial saliva. The procedure was repeated daily for 30 consecutive days. The enamel specimens were kept in the lab oven throughout the duration of the experiment and were removed only for MI paste application and rinsing procedures.

Baseline color and surface profilometry measurements were made for all 50 enamel blocks. The facial surface of each block was measured at baseline, immediately after accelerated demineralization and after 3 and 30 days of storage for color stability and surface morphologies.

The artificial saliva was prepared according to the formulation of ElSayad et al and consisted of 0.4 g NaCl, 0.4 g KCl, 0.6 g $CaCl_2$, 0.6 g NaH_2PO_4, 4 g urea, 4 g Mucin, 0.0016 g Na_2S, 0.0016 g $Mg_2P_2O_7$, and 1 L distilled water at oral temperature at 37°C (ElSayad et al 2009).

Color Stability:

Color was measured using a spectrophotometer (VITA Easyshade, Vident, Brea, CA) set to the CIELAB color-notation system. Specimens were rinsed with distilled water. Three measurements were made per specimen. The spectrophotometer provided Commission Internationale de l'Éclairage (CIE) color space values for lightness (L^*), green-red (a^*) and blue-yellow (b^*). Changes in L^* were calculated between baseline and 30 days post-treatment. A mean Delta L* and standard deviation were determined per group.

Surface Profilometry:

The specimens were evaluated using a non-contact, optical profilometer (ProScan 2000, Scantron, Taunton, UK). Surface parameters roughness and waviness were evaluated. Specimens were demarcated with reference marks to allow triangulation and realignment to allow surface profile determination using analysis software (Pro Form, Scantron). Changes in Sm were calculated between baseline and 30 days post-treatment. Mean values for Ra, Sm, and Delta Sm and their respective standard deviation were determined per group.

Table 1: Study Materials

Material Name	Type	Manufacturer	Composition
ICON	Resin Infiltrant	DMG, Englewood, NJ, USA	Infiltrant: Triethylene-Glycol-Dimethacrylate-Based Resin Etch: 15% HCl, Water, Pyrogenic Silica, Tenside, Pigments Dry: Ethanol
MI Paste™	Recaldent™ (CPP-ACP)	GC America, Alsip, IL, USA	Water, Glycerol, CPP-ACP, D-Sorbitol, CMC-Na, Propylene Glycol, Silicon Dioxide, Titanium Dioxide, Xylitol, Phosphoric Acid, Zinc Oxide, Sodium Saccharin, Ethyl p-Hydroxybenzoate, Magnesium Oxide, Guar Gum, Propyl p-Hydroxybenzoate, Butyl p-Hydroxybenzoate

Table 2: Study Groupings

Groups 50 Enamel Blocks (4 x 4 mm^2)	Treatment	Storage Medium	Baseline Evaluation	Demineralization	Surface Evaluation (3 Days and 30 Days)
1 (Control-Saliva)	None	Saliva	Color and surface profilometry measurements	Creation of accelerated surface mineral loss using 1M HCl (pH 1.5) for 2 minutes	Color and surface profilometry measurements
2 (ICON-Saliva)	ICON	Saliva			
3 (MIP-Saliva)	MI Paste (CCP-ACP)	Saliva			
4 (ICON-Water)	ICON	Water			
5 (MIP-Humidity)	MI Paste CCP-ACP	100% Humidity			

C.   Statistical Management of Data

The means and standard deviations of Ra, Sm, Delta L*, and Delta Sm were tabulated for each group and analyzed by one-way analysis of variance (ANOVA, alpha = 0.05).   The Tukey-Kramer multiple comparison procedure was used for post hoc comparisons.

IV. RESULTS

Significant differences in Delta L* over 30 days were found between the groups (p<0.05). Groups 2, 3, and 4 returned to baseline values over 30 days. Groups 1 and 5 did not return to the baseline values over the 30 days (see Figure 1).

Significant changes were observed in Ra (p<0.05). The average Ra values for Group 1, 3, and 5 after demineralization were less than the average baseline Ra values prior to demineralization and never returned to the baseline values over the 30 days. There was no significant change in group 2. Group 4 values were less than baseline values after demineralization then rose above baseline values after 30 days (see Figure 2).

Significant changes occurred with Sm amongst the groups (p<0.05). Groups 2, 3, and 4 returned to baseline values. Group 5 did not show a significant change following MI paste treatment (see Figure 3).

Significant changes occurred in delta Sm over the 30 days (p<0.05). Groups 1, 2, and 3 followed a deceasing pattern of change. Groups 2, 3, and 4 also followed a similar pattern of change as did groups 1 and 5. The correlation in delta Sm between the groups is observable (see figure 4) and will be discussed further.

Figure 1
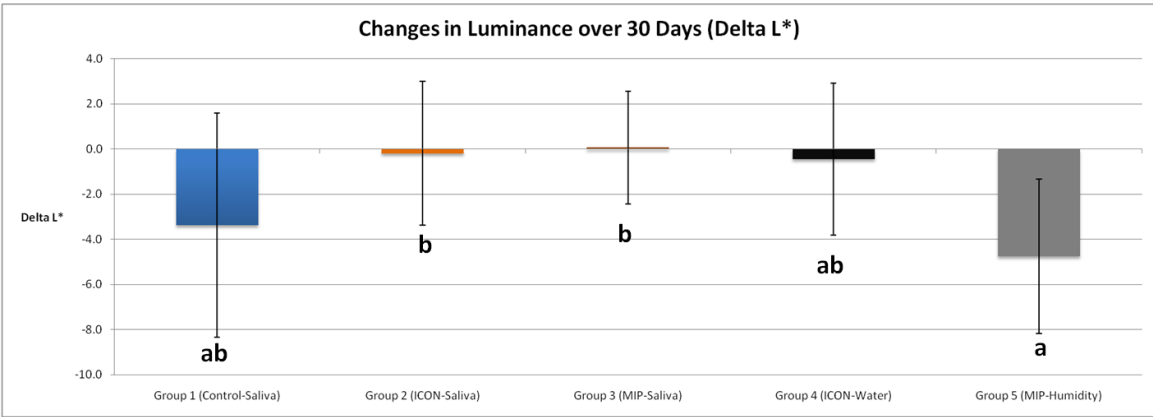
Figure 2
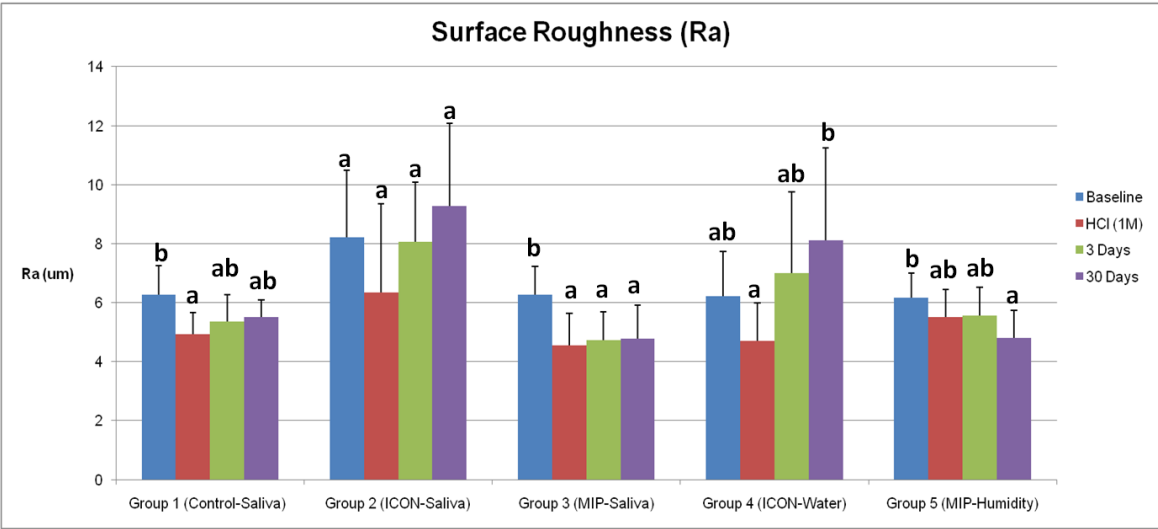
Figure 3
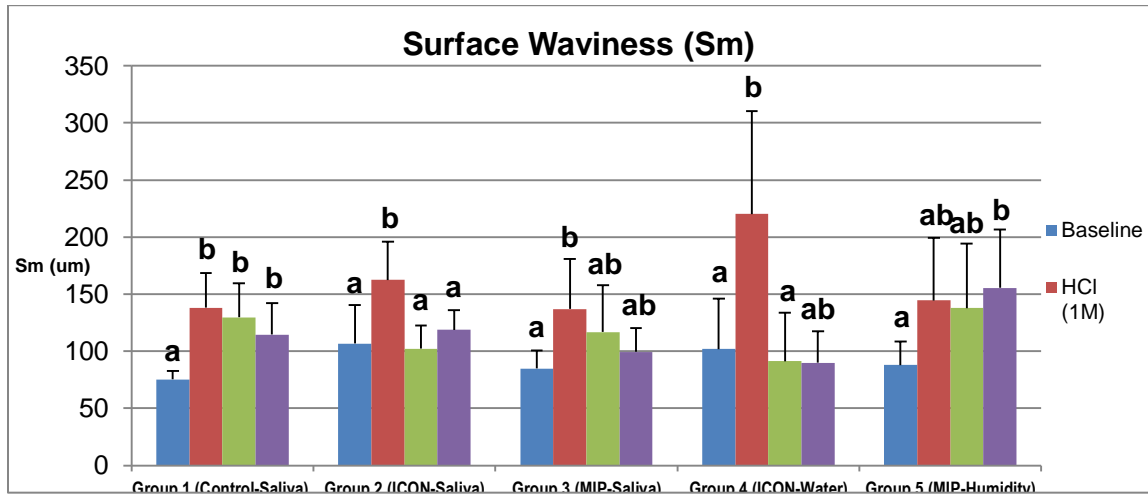
Figure 4
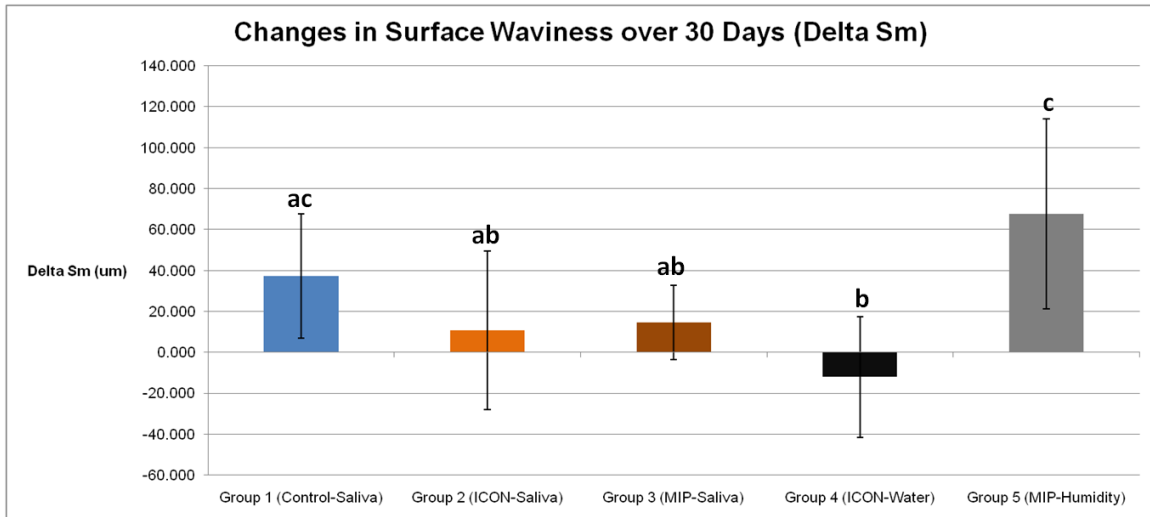
V.   DISCUSSION

Color Discussion:

The first null hypothesis was rejected. There was a significant difference in color stability of enamel blocks whose surfaces were modified to simulate accelerated mineral loss when treated with resin infiltration or MIP paste. Since ICON has a greater ability to restore the color of an enamel block treated with accelerated mineral loss to its original color than MI paste regardless of the storage medium, the first alternative hypothesis was not rejected. In addition MI paste did not show a greater ability to restore the color of an enamel block treated with accelerated mineral loss to its original color than ICON. The third alternative hypothesis was rejected.

In this study, the CIE system was applied to characterize the enamel colors. Three parameters were used to map the enamel photometric properties: a luminance (L^*) and two color coordinates (a^* and b^*) which specified the point on the chromaticity. The L^* value measured the luminous intensity that was emitted or reflected from an enamel block and ranged from 0 (black) to 100 (white). The luminance of an enamel block depends on the internal materials characteristics and surface morphology. For example, like past studies, we noted that the L^* parameter best characterized the surface behavior of demineralization (Torres et al 2011). Since carious lesions undergo changes in mineral density, crystal size, and enamel prism orientation, the deep porosities that were formed from demineralization beneath the non-cavitated surface readily altered the optical scattering property. Unlike sound enamel in which the luminance (L^*) was lowered owing to a lower number of photons entering beyond the enamel to generate backscattering from the underlying enamel prisms, unhealthy hydroxyapatite with accelerated mineral loss impinged and scattered light as photons exited the surface in random directions (Ko et al 2000). The result was a diffuse spectra leading to a higher L^* value and the appearances of a chalky white

spot.   Further, it has been verified that the L* value showed an increase after demineralization (Oikarinen et al 1994).

By analyzing delta L* values, we found significant differences in optical contrast between our experimental groups. Group 1 and Group 5 showed significant delta L* change and did not recover to the baseline color over the 30-day period. From our earlier discussion regarding diffuse reflection, the delta L* value for Group 1 was supposed to produce a positive change indicating a rise in whiteness, an outcome of the random scattering of light paths due to demineralization. Although the whiteness color was immediately observed after 1 molar HCl application and after soaking in saliva for 30 days, a significant negative change in delta L* value (staining) was observed. We suspected the non-sterile artificial saliva could have contributed to the decreasing delta L* values. Because the surface was microscopically eroded by a strong acid, the defective hydroxylapatites were perhaps more susceptible to collect microbes from the non-sterile artificial saliva solution.   As previously demonstrated by (Hosoya et al 2003), after bleaching, the enamel surface was vulnerable to adhesion of *Streptococcus mutans*. The MI paste treated enamel blocks in Group 3 were also soaked in saliva, but we hypothesized that the antimicrobial ingredients of MI paste such as titanium dioxide and xylitol might impede microbial growths in the non-sterile artificial saliva solution.

Furthermore, the difference in delta L* values between Group 1, Group 3, and Group 5 might be linked to the bathing media used for saturating each group. Numerous studies have supported the use of MI paste to treat a demineralized tooth surface and have shown that MI paste in saliva could act as a calcium phosphate reservoir (Reynolds et al 1995, 1997, 1987, 1998). We suspected that for Group 5, the 100% humidity medium did not offer the proper saturating conditions for encouraging CPP to stabilize calcium phosphate and to form small CPP-ACP clusters.   For remineralization to occur, the 100% humidity medium had to preserve a supersaturated mineral environment that acted as a calcium and phosphate

reservoir. Without the molarity difference between demineralized enamel and the supersaturated reservoir, the osmotic gradient could not be readily created to force demineralization to remineralization (ten Cate 2001). However, to date, no study has shown a positive increase in delta L* value after MI paste application or a correlation between enamel surface color after successful MIP therapy with remineralization.

Groups 2 and 4 indicated that resin infiltration was effective in returning the color of demineralized tooth to its original color. In a similar study, treatment with ICON was compared to fluoride therapy, and ICON was able to mask the white spot lesions by infiltration into the porously demineralized hydroxyapatite structures (Torres et al 2011). According to Paris et al (2009), the porosities within the non-cavitated lesions were infiltrated with resin instead of water and air. Since resin was reported to have a refractive index that was similar to enamel than water or air, the difference between resin-infiltrated porosities and enamel refractive indices were minimized. The affected lesions regained translucency and appeared similar to the surrounding enamel (Paris et al 2009; Peters et al 2010).

Surface Topography Discussion:

The second null hypothesis was rejected. Our experiment has demonstrated that there is a significant difference in surface morphology of enamel blocks whose surfaces are modified to simulate accelerated mineral loss when treated with resin infiltration or MI paste. Since ICON has a greater ability to restore the surface of an enamel block treated with accelerated mineral loss to its original morphology than MI paste regardless of the storage medium, the second alternative hypothesis was not rejected. In addition, MI paste did not show a greater ability to restore the surface of an enamel block treated with accelerated mineral loss to its original morphology than ICON. The fourth alternative hypothesis was rejected.

In this study, topography of the enamel surface played an important role in determining the responses for de- and re-mineralization. One of the most important topographic properties was surface roughness (Ra). Ra was defined as closely spaced irregularities, protuberances, or ridges; and, average Ra was the arithmetic average of the absolute values of the roughness profile ordinates. The average Ra provided good overall description of height variations but was not a good discriminator for different types of surfaces. No distinction could be made between peaks and valleys. Another parameter, the mean spacing of adjacent local peaks (Sm) or waviness was applied to measure the highest part of the profile calculated between two adjacent minima. Ra and Sm values assessed the surface profiles for deviations which could indirectly influence the amount of light scattering and color stability. However, Ra and Sm parameters contained no information about the rate of wear and the potential of a surface to retain fluids or to absorb substances. By analyzing the Ra and Sm values, we found significant differences in surface profiles between our experimental groups. Furthermore, our data indicated a correlation between the waviness parameter and color stability.

Typically, Ra was reported since this value plays an important role in determining how a surface will interact with abrasion, attrition, and erosion. Past studies have shown that after acid etching or bleaching, a significant increase of enamel Ra was observed (Hosoya et al 2003; Barkmeier et al 2009). In this study, a significant increase in Ra after etching was not observed for Group 2, 4, and 5, but a significant decrease in Ra after MI paste therapy was observed for Group 3 and 5. Furthermore, no significant increase in Ra between before and after ICON therapy was noted for Group 2 and 4. Conceptually, the purpose of ICON was to infiltrate into the porous body of a non-cavitated incipient lesion, thereby arresting the lesion and returning the surface morphologies like roughness and waviness characteristics back to normal. Because we were unable to produce a significant Ra difference between sound enamel and acid-challenged enamel, our Ra data failed to predict the efficacy of ICON on demineralized enamel surfaces. However, our result has

directly demonstrated that the roughness of an unpolished ICON layer was significantly similar to the roughness of an enamel surface with and without the presence of acidic abuses. Our results for group 2 and 4 were similar to a recent study that has also found no significant differences in Ra values between before and after application of ICON to sound enamel surfaces (Taher et al 2011). Also, Burgess and Cakir (2010) measured the Ra values of four groups (sound enamel, polished resin-infiltrated enamel, resin-infiltrated enamel, and carious enamel) and concluded that no significant differences in Ra were found between the aforementioned four groups.

One limitation of this study involved the ability to image surface topography accurately. Significant quantification of surface characteristics like Ra and Sm depended on the lateral spatial resolution of the profilometer's chromatic pen. Lateral spatial resolution was defined as the ability of a system to distinguish significantly between two closely adjacent surface points. For our chromatic pen (CL-MG 20 16/2.5, STIL, France), the smallest spatial interval that can be reproduced was approximately seven micrometers. Ra was considered to be the high frequency, short wavelength component of a measured surface. The wavelength of Ra was considerably less than our lateral spatial resolution and our system could not discern true signals from the ambient noises, leading to a poor signal-to-noise ratio. However, using the same profilometer (ProScan 2000), Barkmeier et al (2009) have reported that the human enamel Ra values after acidic etching were in the range of 0.1 – 0.5 micrometer, and Burgess and Cakir (2010) have reported that the healthy human enamel Ra values were in the range of 40 – 50 micrometers. This wide range of enamel Ra values could be related to the different chromatic pens that were used in each of the two previous studies. Furthermore, a cut-off filter of 0.25 mm was applied in the Barkmeier et al (2009) study, but a cut-off filter of 0.08 mm was used in the Burgess and Cakir (2010) study. According to the International Organization for Standardization, the cut-off filter has a huge impact on the measurement of Ra and Sm, and selecting a small

cut-off filter would result in a small roughness values. For future study, we recommended a profilometer with a lateral spatial resolution in the range of 10 – 500 nanometers.

By analyzing Sm values, we found significant differences in surface waviness between our experimental groups. In our study, the Sm values for groups 2, 3, 4 rose significantly after demineralization and returned to near the baseline value after 30 days. The Sm values in groups 1 and 5 rose significantly following demineralization but did not return to their baseline values. This trend would be expected for the control group with no treatment. Groups 2 and 4 intuitively returned to baseline because ICON infiltrated into the porous body of the non-cavitated incipient lesion and arrested the lesion returning the surface morphologies back to normal. It is suspected that Group 3 returned to baseline because the MI paste in saliva acts as a calcium phosphate reservoir, buffering the free calcium and phosphate ion activities, thereby helping to maintain a state of supersaturation with respect to tooth mineral, depressing enamel demineralization, and enhancing remineralization (Reynolds 1995, 1997, 1987, 1998). This may also explain why group 5 did not return to baseline because the medium it was stored in did not support the minerals necessary to promote remineralization (Reynolds 1997). Since luminosity of a material depends highly on the reflectivity or characteristics of the material surface, a correlation between delta L* and delta Sm was suspected. Groups 2, 3, and 4 all changed significantly after etching and returned to the baseline value after treatment when observed for 30 days. Groups 1 and 5 did not return to baseline over the 30 day period. This suspected correlation has to do with the relationship between luminosity and surface characteristics. The rougher that a material surface is means it will be less reflective. In our case, it appears that groups 1 and 5 may be rougher with the result that they are less reflective in comparison to the other groups.

Since the Ra values in this study were inconclusive, for future studies, the following changes could be considered to remedy the problems that were encountered. One, problems with the Proscan's inability to distinguish spatial intervals lesser than 7 microns could be possibly resolved by using an atomic force microscopy or a newer 3D optical device like the Contour GT, which could accommodate submicron resolutions. Furthermore, the questionable reliability and accuracy to measure surface profiles were complicated by the frequent breakdowns of the Proscan. Second, our initial intent for using a mild (lactic) acid did not generate a clinically representative white spot lesion due to repeated fungal contamination that rendered our lactic acid solution unusable. Finally, without another comparable substitute, the strong acid used for demineralization eroded the enamel surface much more rapidly and aggressively than simply creating a white spot lesion.

VI.   CONCLUSION

The results of the present study do not provide conclusive evidence that the standard of care for enamel demineralization and potential remineralization should shift towards the application of ICON or MI Paste™ / Plus™ technologies, even though significant differences in Delta L* and Sm values between ICON treated group and control group were noted.   Unfortunately, the values for surface roughness were inconclusive; thereby, rendering obscurity to make a clinical recommendation.

VII. Appendix

Change in Surface Waviness   Change in Luminance

		Delta Sm					Delta L		
1	C-S	83.864			1	C-S	-1.7		
2	C-S	13.915			2	C-S	-2.0		
3	C-S	20.571			3	C-S	-2.6		
4	C-S	94.788			4	C-S	0.2		
5	C-S	10.001			5	C-S	-2.3		
6	C-S	27.664			6	C-S	1.9		
7	C-S	23.984			7	C-S	-5.1		
8	C-S	33.686	C-S Ave	37.323	8	C-S	-5.5		
9	C-S	27.435	C-S Stdev	30.466	9	C-S	-16.0	C-S Ave	-3.4
1	ICON-S	-44.087			10	C-S	-0.7	C-S Stdev	5.0
2	ICON-S	28.642			1	ICON-S	-1.7		
3	ICON-S	14.362			2	ICON-S	2.3		
4	ICON-S	73.386			3	ICON-S	3.0		
5	ICON-S	19.597			4	ICON-S	0.4		
6	ICON-S	-42.426			5	ICON-S	2.7		
7	ICON-S	6.587	ICON-S Ave	10.733	6	ICON-S	-1.4		
8	ICON-S	29.804	ICON-S Stdev	38.822	7	ICON-S	-1.1		
1	ICON-W	-30.961			8	ICON-S	-2.1		
2	ICON-W	0.162			9	ICON-S	3.1	ICON-S Ave	-0.2
3	ICON-W	-72.890			10	ICON-S	-7.1	ICON-S Stdev	3.2
4	ICON-W	9.308			1	ICON-W	3.9		
5	ICON-W	-17.647			2	ICON-W	-0.1		
6	ICON-W	42.255			3	ICON-W	0.1		

7	ICON-W	-1.735			4	ICON-W	-0.9		
8	ICON-W	-11.520			5	ICON-W	4.9		
9	ICON-W	-20.997	ICON-W Ave	-12.095	6	ICON-W	-2.2		
10	ICON-W	-16.922	ICON-W Stdev	29.543	7	ICON-W	-6.4		
1	MIP-S	-5.288			8	ICON-W	1.4		
2	MIP-S	2.077			9	ICON-W	-3.7	ICON-W Ave	-0.5
3	MIP-S	16.447			10	ICON-W	-1.5	ICON-W Stdev	3.4
4	MIP-S	15.250			1	MIP-S	1.4		
5	MIP-S	23.013			2	MIP-S	1.2		
6	MIP-S	32.877			3	MIP-S	2.2		
7	MIP-S	23.301			4	MIP-S	-5.3		
8	MIP-S	36.833			5	MIP-S	-2.7		
9	MIP-S	-22.405	MIP-S Ave	14.439	6	MIP-S	2.9		
10	MIP-S	22.289	MIP-S Stdev	18.133	7	MIP-S	0.4		
1	MIP-W	41.77			8	MIP-S	-0.8		
2	MIP-W	58.958			9	MIP-S	1.7	MIP-S Ave	0.1
3	MIP-W	58.162			10	MIP-S	-0.4	MIP-S Stdev	2.5
4	MIP-W	16.473			1	MIP-W	-4.5		
5	MIP-W	133.399			2	MIP-W	-0.8		
6	MIP-W	69.104			3	MIP-W	-0.6		
7	MIP-W	138.856			4	MIP-W	-5.9		
8	MIP-W	102.952			5	MIP-W	-6.3		
9	MIP-W	-4.597	MIP-W Ave	67.511	6	MIP-W	-6.3		
10	MIP-W	60.037	MIP-W Stdev	46.396	7	MIP-W	-12.4		
					8	MIP-W	-5.2		
					9	MIP-W	-2.5	MIP-W Ave	-4.7
					10	MIP-W	-3.2	MIP-W Stdev	3.4

Surface Topography

Group 1 control-saliva baseline

		a	b	c	Ave
1	ISO Am	46.214	51.392	33.372	43.659
	ISO Ra	5.281	5.766	5.919	5.655
	ISO Sm	61.326	75.094	68.765	68.395
	ISO Wt	147.912	133.365	104.910	128.729
	ISO Rmax	115.033	102.744	93.229	103.669
	ISO Rv	46.214	51.392	33.372	43.659
	ISO Rz	51.670	49.640	43.809	48.373

2	ISO Am	44.849	43.615	38.364	42.276
	ISO Ra	7.227	7.146	6.371	6.915
	ISO Sm	89.314	66.208	66.398	73.973
	ISO Wt	65.044	87.453	77.189	76.562
	ISO Rmax	59.320	87.453	77.189	74.654
	ISO Rv	44.849	43.615	38.364	42.276
	ISO Rz	43.393	48.411	45.670	45.825

3	ISO Am	68.244	68.907	85.985	74.379
	ISO Ra	6.973	6.759	6.456	6.729
	ISO Sm	69.644	69.805	68.324	69.258
	ISO Wt	135.540	138.310	173.094	148.981
	ISO Rmax	135.540	138.310	173.094	148.981
	ISO Rv	68.244	68.907	85.985	74.379
	ISO Rz	51.575	52.622	56.509	53.569

4	ISO Am	27.441	33.968	35.952	32.454
	ISO Ra	4.796	4.761	5.447	5.001
	ISO Sm	94.147	56.260	68.653	73.020
	ISO Wt	54.295	51.428	54.819	53.514
	ISO Rmax	54.295	35.519	49.175	46.330
	ISO Rv	27.441	33.968	35.952	32.454
	ISO Rz	33.712	34.406	35.656	34.591

5	ISO Am	44.944	42.699	57.180	48.274
	ISO Ra	5.975	5.544	5.827	5.782
	ISO Sm	75.549	69.885	61.914	69.116
	ISO Wt	83.279	85.428	113.568	94.092
	ISO Rmax	83.279	85.428	113.568	94.092
	ISO Rv	44.944	42.699	57.180	48.274
	ISO Rz	41.310	39.389	43.724	41.474

6	ISO Am	67.333	62.441	58.349	62.708
	ISO Ra	8.673	8.231	8.013	8.306
	ISO Sm	76.179	77.086	83.363	78.876
	ISO Wt	145.285	124.056	117.504	128.948
	ISO Rmax	143.925	124.056	117.504	128.495
	ISO Rv	67.333	62.441	58.349	62.708
	ISO Rz	63.396	55.575	52.064	57.012

7	ISO Am	55.528	41.534	48.335	48.466
	ISO Ra	6.479	6.205	6.584	6.423
	ISO Sm	69.050	73.621	71.586	71.419
	ISO Wt	72.354	59.730	71.735	67.940
	ISO Rmax	46.137	50.495	53.016	49.883
	ISO Rv	55.528	41.534	48.335	48.466
	ISO Rz	38.044	34.167	40.138	37.450

8	ISO Am	36.191	23.417	33.885	31.164
	ISO Ra	5.132	5.098	5.267	5.166
	ISO Sm	84.480	100.921	95.341	93.581
	ISO Wt	50.669	38.105	50.318	46.364
	ISO Rmax	50.363	36.073	39.762	42.066
	ISO Rv	36.191	23.417	33.885	31.164
	ISO Rz	30.430	30.465	31.577	30.824

9	ISO Am	29.731	52.292	36.721	39.581
	ISO Ra	7.185	6.624	6.652	6.820
	ISO Sm	76.030	85.830	71.089	77.650
	ISO Wt	50.840	74.970	54.934	60.248
	ISO Rmax	48.122	74.970	51.435	58.176
	ISO Rv	29.731	52.292	36.721	39.581
	ISO Rz	41.507	44.818	41.318	42.548

10	ISO Am	43.990	38.992	46.649	43.210
	ISO Ra	6.214	6.513	5.260	5.996
	ISO Sm	81.030	78.275	78.077	79.127
	ISO Wt	64.643	65.550	69.576	66.590
	ISO Rmax	40.441	44.099	24.872	36.471
	ISO Rv	43.990	38.992	46.649	43.210
	ISO Rz	38.378	38.715	32.476	36.523

Average Surface Topography

Group 1 control-saliva baseline

	1	2	3	4	5	6	7	8	9	10	Ave	STDEV
ISO Am	43.659	42.276	74.379	32.454	48.274	62.708	48.466	31.164	39.581	43.210	46.617	13.182
ISO Ra	5.655	6.915	6.729	5.001	5.782	8.306	6.423	5.166	6.820	5.996	6.279	0.978
ISO Sm	68.395	73.973	69.258	73.020	69.116	78.876	71.419	93.581	77.650	79.127	75.441	7.538
ISO Wt	128.729	76.562	148.981	53.514	94.092	128.948	67.940	46.364	60.248	66.590	87.197	36.163
ISO Rmax	103.669	74.654	148.981	46.330	94.092	128.495	49.883	42.066	58.176	36.471	78.282	39.043
ISO Rv	43.659	42.276	74.379	32.454	48.274	62.708	48.466	31.164	39.581	43.210	46.617	13.182
ISO Rz	48.373	45.825	53.569	34.591	41.474	57.012	37.450	30.824	42.548	36.523	42.819	8.425

Surface Topography

Group 1 control-saliva demineralization

		a	b	c	Ave
1	ISO Am	35.248	38.050	35.211	36.170
	ISO Ra	4.282	4.607	4.412	4.434
	ISO Sm	104.826	113.423	146.662	121.637
	ISO Wt	45.971	111.955	98.718	85.548
	ISO Rmax	23.191	89.862	74.746	62.600
	ISO Rv	35.248	38.050	35.211	36.170
	ISO Rz	23.297	37.198	32.624	31.040

		a	b	c	Ave
2	ISO Am	46.650	52.781	50.910	50.114
	ISO Ra	5.504	5.653	5.952	5.703
	ISO Sm	120.977	115.940	163.653	133.523
	ISO Wt	62.846	67.383	65.048	65.092
	ISO Rmax	56.180	65.766	65.048	62.331
	ISO Rv	46.650	52.781	50.910	50.114
	ISO Rz	32.134	35.303	32.863	33.433

		a	b	c	Ave
3	ISO Am	66.336	67.492	65.102	66.310
	ISO Ra	4.360	4.416	4.356	4.377
	ISO Sm	238.238	201.432	191.216	210.295
	ISO Wt	75.748	75.005	72.592	74.448
	ISO Rmax	75.748	75.005	72.592	74.448
	ISO Rv	66.336	67.492	65.102	66.310
	ISO Rz	24.583	24.658	23.447	24.229

		a	b	c	Ave
4	ISO Am	29.153	33.104	31.521	31.259
	ISO Ra	4.751	4.134	4.666	4.517
	ISO Sm	148.121	143.220	128.642	139.994
	ISO Wt	45.013	66.306	51.354	54.224
	ISO Rmax	45.013	66.306	44.278	51.866
	ISO Rv	29.153	33.104	31.521	31.259
	ISO Rz	23.301	30.077	28.317	27.232

		a	b	c	Ave
5	ISO Am	33.511	36.423	35.797	35.244
	ISO Ra	4.311	4.362	4.344	4.339
	ISO Sm	169.913	158.918	115.309	148.047
	ISO Wt	43.196	47.053	45.311	45.187
	ISO Rmax	39.160	41.773	42.141	41.025
	ISO Rv	33.511	36.423	35.797	35.244
	ISO Rz	20.992	22.080	22.964	22.012

6	ISO Am	46.366	32.188	33.735	37.430
	ISO Ra	6.147	5.239	4.397	5.261
	ISO Sm	134.752	126.707	110.147	123.869
	ISO Wt	59.858	45.179	45.907	50.315
	ISO Rmax	41.892	37.553	35.052	38.166
	ISO Rv	46.366	32.188	33.735	37.430
	ISO Rz	28.486	25.174	24.079	25.913

7	ISO Am	47.469	52.595	49.940	50.001
	ISO Ra	5.585	5.639	5.881	5.702
	ISO Sm	100.221	97.304	98.585	98.703
	ISO Wt	65.857	191.554	68.021	108.477
	ISO Rmax	37.855	167.768	49.019	84.881
	ISO Rv	47.469	52.595	49.940	50.001
	ISO Rz	32.318	59.287	34.897	42.167

8	ISO Am	29.573	45.886	49.872	41.777
	ISO Ra	4.491	5.848	6.039	5.459
	ISO Sm	128.933	132.706	161.851	141.163
	ISO Wt	42.430	108.450	63.111	71.330
	ISO Rmax	29.746	80.798	25.969	45.504
	ISO Rv	29.573	45.886	49.872	41.777
	ISO Rz	24.914	41.275	28.983	31.724

9	ISO Am	22.506	23.262	30.312	25.360
	ISO Ra	4.019	3.551	3.773	3.781
	ISO Sm	169.821	134.484	151.582	151.962
	ISO Wt	30.531	32.731	44.164	35.809
	ISO Rmax	28.785	21.812	24.071	24.889
	ISO Rv	22.506	23.262	30.312	25.360
	ISO Rz	17.966	17.962	20.585	18.838

10	ISO Am	39.135	35.665	37.855	37.552
	ISO Ra	6.183	6.054	5.041	5.759
	ISO Sm	108.109	145.482	86.812	113.468
	ISO Wt	58.610	56.288	53.813	56.237
	ISO Rmax	58.610	46.039	36.284	46.978
	ISO Rv	39.135	35.665	37.855	37.552
	ISO Rz	33.025	33.983	29.967	32.325

Average Surface Topography

Group 1 control-saliva demineralization

	1	2	3	4	5	6	7	8	9	10	Ave	STDEV
ISO Am	36.170	50.114	66.310	31.259	35.244	37.430	50.001	41.777	25.360	37.552	41.122	11.670
ISO Ra	4.434	5.703	4.377	4.517	4.339	5.261	5.702	5.459	3.781	5.759	4.933	0.720
ISO Sm	121.637	133.523	210.295	139.994	148.047	123.869	98.703	141.163	151.962	113.468	138.266	30.128
ISO Wt	85.548	65.092	74.448	54.224	45.187	50.315	108.477	71.330	35.809	56.237	64.667	21.328
ISO Rmax	62.600	62.331	74.448	51.866	41.025	38.166	84.881	45.504	24.889	46.978	53.269	17.958
ISO Rv	36.170	50.114	66.310	31.259	35.244	37.430	50.001	41.777	25.360	37.552	41.122	11.670
ISO Rz	31.040	33.433	24.229	27.232	22.012	25.913	42.167	31.724	18.838	32.325	28.891	6.692

Surface Topography

Group 1 control-saliva 30 days

		a	b	c	Ave					
1	ISO Am	36.531	39.126	33.378	36.345					
	ISO Ra	4.463	3.628	4.052	4.048					
	ISO Sm	190.715	104.280	125.048	140.014					
	ISO Wt	52.223	50.176	48.927	50.442					
	ISO Rmax	29.184	25.940	22.155	25.760					
	ISO Rv	36.531	39.126	33.378	36.345					
	ISO Rz	24.423	23.420	24.792	24.212					
2	ISO Am	51.105	47.945	48.599	49.216					
	ISO Ra	6.165	6.357	6.170	6.231					
	ISO Sm	183.907	108.305	108.065	133.426					
	ISO Wt	67.815	64.300	64.344	65.486					
	ISO Rmax	64.916	58.708	58.656	60.760					
	ISO Rv	51.105	47.945	48.599	49.216					
	ISO Rz	33.602	35.360	33.840	34.267					
				Dropped						
3	ISO Am	72.343	124.099	233.724	143.389		72.343	124.099		98.221
	ISO Ra	6.302	6.710	11.525	8.179		6.302	6.710		6.506
	ISO Sm	136.713	148.144	476.755	253.871		136.713	148.144		142.429
	ISO Wt	82.283	137.787	292.440	170.837		82.283	137.787		110.035
	ISO Rmax	82.157	135.440	292.440	170.012		82.157	135.440		108.799
	ISO Rv	72.343	124.099	233.724	143.389		72.343	124.099		98.221
	ISO Rz	29.186	43.010	72.666	48.287		29.186	43.010		36.098
4	ISO Am	21.390	31.200	31.566	28.052					
	ISO Ra	4.667	4.422	4.492	4.527					
	ISO Sm	163.360	165.665	136.556	155.194					
	ISO Wt	37.928	41.892	42.753	40.858					
	ISO Rmax	33.749	41.892	40.619	38.753					
	ISO Rv	21.390	31.200	31.566	28.052					
	ISO Rz	22.904	24.308	25.204	24.139					
5	ISO Am	40.273	40.007	52.895	44.392					
	ISO Ra	4.367	4.448	4.825	4.547					
	ISO Sm	89.900	78.057	68.263	78.740					
	ISO Wt	54.254	52.939	64.213	57.135					
	ISO Rmax	37.873	43.407	63.064	48.115					
	ISO Rv	40.273	40.007	52.895	44.392					
	ISO Rz	26.134	28.553	31.135	28.607					

6	ISO Am	73.806	65.567	64.972	68.115
	ISO Ra	7.313	7.328	7.051	7.231
	ISO Sm	159.977	179.241	155.372	164.863
	ISO Wt	89.603	84.644	80.391	84.879
	ISO Rmax	84.802	79.609	80.391	81.601
	ISO Rv	73.806	65.567	64.972	68.115
	ISO Rz	39.424	38.782	38.846	39.017

7	ISO Am	51.047	47.958	52.213	50.406
	ISO Ra	5.357	5.539	5.599	5.498
	ISO Sm	71.219	96.951	83.215	83.795
	ISO Wt	77.003	63.316	69.467	69.929
	ISO Rmax	33.261	42.396	45.382	40.346
	ISO Rv	51.047	47.958	52.213	50.406
	ISO Rz	35.761	30.395	33.130	33.095

8	ISO Am	60.144	53.073	55.970	56.396
	ISO Ra	5.450	5.661	5.737	5.616
	ISO Sm	148.272	155.160	140.554	147.995
	ISO Wt	77.469	66.448	74.269	72.729
	ISO Rmax	69.688	63.538	74.269	69.165
	ISO Rv	60.144	53.073	55.970	56.396
	ISO Rz	32.929	32.627	33.981	33.179

9	ISO Am	21.884	21.720	29.490	24.365
	ISO Ra	5.322	5.084	4.629	5.012
	ISO Sm	174.912	157.131	118.083	150.042
	ISO Wt	35.478	34.367	43.418	37.754
	ISO Rmax	35.132	34.178	33.761	34.357
	ISO Rv	21.884	21.720	29.490	24.365
	ISO Rz	27.222	26.642	25.345	26.403

10	ISO Am	33.097	28.591	28.154	29.947
	ISO Ra	5.986	5.769	5.139	5.631
	ISO Sm	121.474	119.801	78.472	106.582
	ISO Wt	50.346	43.789	50.219	48.118
	ISO Rmax	50.063	37.517	39.407	42.329
	ISO Rv	33.097	28.591	28.154	29.947
	ISO Rz	33.926	31.638	30.889	32.151

Average Surface Topography

Group 1 control-saliva 30 days

	1	2	3	4	5	6	7	8	9	10	Ave	STDEV
ISO Am	36.345	49.216	42.781	28.052	44.392	68.115	50.406	56.396	24.365	29.947	43.001	13.708
ISO Ra	4.048	6.231	5.139	4.527	4.547	7.231	5.498	5.616	5.012	5.631	5.348	0.923
ISO Sm	140.014	133.426	136.720	155.194	78.740	164.863	83.795	147.995	150.042	106.582	129.737	29.894
ISO Wt	50.442	65.486	57.964	40.858	57.135	84.879	69.929	72.729	37.754	48.118	58.529	14.886
ISO Rmax	25.760	60.760	43.260	38.753	48.115	81.601	40.346	69.165	34.357	42.329	48.445	17.053
ISO Rv	36.345	49.216	42.781	28.052	44.392	68.115	50.406	56.396	24.365	29.947	43.001	13.708
ISO Rz	24.212	34.267	29.240	24.139	28.607	39.017	33.095	33.179	26.403	32.151	30.431	4.776

Surface Topography

Group 2 icon-saliva baseline

		a	b	c	Ave
1	ISO Am	79.017	68.096	70.961	72.691
	ISO Ra	11.462	11.169	11.728	11.453
	ISO Sm	109.389	127.617	154.433	130.480
	ISO Wt	153.952	111.392	100.980	122.108
	ISO Rmax	97.597	93.909	88.515	93.340
	ISO Rv	79.017	68.096	70.961	72.691
	ISO Rz	62.331	51.829	56.104	56.755

2	ISO Am	90.630	89.130	70.448	83.403
	ISO Ra	10.241	9.360	9.511	9.704
	ISO Sm	167.785	150.622	186.952	168.453
	ISO Wt	111.554	111.311	93.235	105.367
	ISO Rmax	88.249	70.521	87.274	82.015
	ISO Rv	90.630	89.130	70.448	83.403
	ISO Rz	51.293	49.691	45.457	48.814

3	ISO Am	50.541	57.313	52.359	53.404
	ISO Ra	8.072	7.515	7.473	7.687
	ISO Sm	100.272	80.104	97.008	92.461
	ISO Wt	74.169	87.470	74.550	78.730
	ISO Rmax	67.844	82.098	74.550	74.831
	ISO Rv	50.541	57.313	52.359	53.404
	ISO Rz	45.932	48.730	45.580	46.747

4	ISO Am	74.658	57.606	65.299	65.854
	ISO Ra	8.666	6.948	7.504	7.706
	ISO Sm	117.125	93.980	125.153	112.086
	ISO Wt	98.143	78.407	84.019	86.856
	ISO Rmax	69.372	47.412	41.026	52.603
	ISO Rv	74.658	57.606	65.299	65.854
	ISO Rz	55.501	41.027	42.063	46.197

5	ISO Am	48.464	42.797	45.381	45.547
	ISO Ra	5.759	4.948	4.934	5.214
	ISO Sm	68.366	67.373	65.815	67.185
	ISO Wt	64.372	58.008	58.244	60.208
	ISO Rmax	31.139	29.447	28.582	29.723
	ISO Rv	48.464	42.797	45.381	45.547
	ISO Rz	34.476	32.237	29.591	32.101

6	ISO Am	51.672	59.423	61.167	57.421
	ISO Ra	7.360	7.275	6.544	7.060
	ISO Sm	173.743	86.823	88.612	116.393
	ISO Wt	77.668	76.664	78.787	77.706
	ISO Rmax	55.086	60.321	67.304	60.904
	ISO Rv	51.672	59.423	61.167	57.421
	ISO Rz	42.097	44.541	41.712	42.783

7	ISO Am	67.381	62.252	63.679	64.437
	ISO Ra	11.672	10.863	12.907	11.814
	ISO Sm	143.926	144.971	123.857	137.585
	ISO Wt	97.277	96.461	106.024	99.921
	ISO Rmax	82.382	64.831	106.024	84.412
	ISO Rv	67.381	62.252	63.679	64.437
	ISO Rz	61.937	61.039	66.641	63.206

8	ISO Am	33.915	35.420	37.429	35.588
	ISO Ra	4.754	5.221	5.743	5.239
	ISO Sm	65.624	77.765	72.754	72.048
	ISO Wt	49.846	50.074	56.567	52.162
	ISO Rmax	33.193	35.655	48.479	39.109
	ISO Rv	33.915	35.420	37.429	35.588
	ISO Rz	31.677	32.663	39.468	34.603

9	ISO Am	58.946	78.752	72.885	70.194
	ISO Ra	9.370	8.223	8.641	8.745
	ISO Sm	154.920	81.459	80.028	105.469
	ISO Wt	103.888	109.744	114.682	109.438
	ISO Rmax	73.487	94.313	91.652	86.484
	ISO Rv	58.946	78.752	72.885	70.194
	ISO Rz	49.689	54.090	59.153	54.311

10	ISO Am	58.381	66.692	55.197	60.090
	ISO Ra	7.689	7.381	7.559	7.543
	ISO Sm	62.792	67.802	66.922	65.839
	ISO Wt	87.420	95.678	84.233	89.110
	ISO Rmax	77.067	85.326	73.880	78.758
	ISO Rv	58.381	66.692	55.197	60.090
	ISO Rz	52.002	55.166	52.515	53.228

Average Surface Topography

Group 2 icon-saliva baseline

	1	2	3	4	5	6	7	8	9	10	Ave	STDEV
ISO Am	72.691	83.403	53.404	65.854	45.547	57.421	64.437	35.588	70.194	60.090	60.863	13.801
ISO Ra	11.453	9.704	7.687	7.706	5.214	7.060	11.814	5.239	8.745	7.543	8.216	2.264
ISO Sm	130.480	168.453	92.461	112.086	67.185	116.393	137.585	72.048	105.469	65.839	106.800	33.486
ISO Wt	122.108	105.367	78.730	86.856	60.208	77.706	99.921	52.162	109.438	89.110	88.161	21.903
ISO Rmax	93.340	82.015	74.831	52.603	29.723	60.904	84.412	39.109	86.484	78.758	68.218	21.599
ISO Rv	72.691	83.403	53.404	65.854	45.547	57.421	64.437	35.588	70.194	60.090	60.863	13.801
ISO Rz	56.755	48.814	46.747	46.197	32.101	42.783	63.206	34.603	54.311	53.228	47.874	9.660

Surface Topography

Group 2 icon-saliva demineralization

		a	b	c	Ave
1	ISO Am	78.812	74.544	96.086	83.147
	ISO Ra	12.168	12.791	14.154	13.038
	ISO Sm	168.725	216.331	129.044	171.367
	ISO Wt	158.730	150.431	185.818	164.993
	ISO Rmax	109.960	107.007	157.789	124.919
	ISO Rv	78.812	74.544	96.086	83.147
	ISO Rz	69.571	64.800	85.504	73.292

2	ISO Am	73.784	N/A	N/A	73.784	
	ISO Ra	7.769	N/A	N/A	7.769	Not able to calculate Sm values for sample 2; therefore, other values are not collected
	ISO Sm	127.429	N/A	N/A	127.429	
	ISO Wt	83.598	N/A	N/A	83.598	
	ISO Rmax	64.148	N/A	N/A	64.148	
	ISO Rv	73.784	N/A	N/A	73.784	
	ISO Rz	34.047	N/A	N/A	34.047	

3	ISO Am	38.767	30.599	35.427	34.931
	ISO Ra	5.334	4.759	6.096	5.396
	ISO Sm	185.121	142.384	146.397	157.967
	ISO Wt	51.927	44.921	49.377	48.742
	ISO Rmax	46.739	29.906	44.032	40.226
	ISO Rv	38.767	30.599	35.427	34.931
	ISO Rz	25.658	22.319	25.453	24.477

4	ISO Am	52.022	49.925	57.557	53.168
	ISO Ra	7.342	8.152	7.564	7.686
	ISO Sm	163.913	158.859	158.969	160.580
	ISO Wt	67.724	71.940	81.773	73.812
	ISO Rmax	45.474	38.703	35.076	39.751
	ISO Rv	52.022	49.925	57.557	53.168
	ISO Rz	36.353	39.192	41.368	38.971

5	ISO Am	27.864	27.624	29.210	28.233
	ISO Ra	3.250	3.005	2.722	2.992
	ISO Sm	142.755	170.908	133.129	148.931
	ISO Wt	35.696	36.588	36.657	36.314
	ISO Rmax	14.227	12.291	11.011	12.510
	ISO Rv	27.864	27.624	29.210	28.233
	ISO Rz	16.997	16.148	14.771	15.972

6	ISO Am	45.214	49.244	49.296	47.918
	ISO Ra	6.223	6.386	6.365	6.325
	ISO Sm	160.063	142.826	172.237	158.375
	ISO Wt	58.642	62.882	62.049	61.191
	ISO Rmax	53.502	54.506	52.462	53.490
	ISO Rv	45.214	49.244	49.296	47.918
	ISO Rz	31.431	33.085	31.865	32.127

7	ISO Am	63.002	55.585	45.909	54.832
	ISO Ra	6.457	8.301	8.208	7.655
	ISO Sm	212.703	276.216	250.412	246.444
	ISO Wt	75.953	74.690	66.945	72.529
	ISO Rmax	32.292	56.291	46.447	45.010
	ISO Rv	63.002	55.585	45.909	54.832
	ISO Rz	31.169	38.458	39.139	36.255

8	ISO Am	16.851	16.913	16.807	16.857
	ISO Ra	3.087	3.184	3.226	3.166
	ISO Sm	150.347	119.770	117.434	129.184
	ISO Wt	24.983	27.721	26.009	26.238
	ISO Rmax	17.606	23.117	21.506	20.743
	ISO Rv	16.851	16.913	16.807	16.857
	ISO Rz	16.994	16.597	17.239	16.943

9	ISO Am	48.837	54.438	55.479	52.918
	ISO Ra	7.207	5.485	5.471	6.054
	ISO Sm	208.555	180.652	135.239	174.815
	ISO Wt	66.254	67.854	74.491	69.533
	ISO Rmax	57.202	63.067	64.596	61.622
	ISO Rv	48.837	54.438	55.479	52.918
	ISO Rz	28.224	25.307	25.910	26.480

10	ISO Am	27.523	29.643	25.016	27.394
	ISO Ra	3.739	3.379	3.031	3.383
	ISO Sm	140.552	173.217	136.195	149.988
	ISO Wt	38.717	40.441	35.748	38.302
	ISO Rmax	32.929	36.159	30.326	33.138
	ISO Rv	27.523	29.643	25.016	27.394
	ISO Rz	19.528	20.275	18.008	19.270

Average Surface Topography

Group 2 icon-saliva demineralization

	1	2	3	4	5	6	7	8	9	10	Ave	STDEV
ISO Am	83.147	73.784	34.931	53.168	28.233	47.918	54.832	16.857	52.918	27.394	47.318	20.947
ISO Ra	13.038	7.769	5.396	7.686	2.992	6.325	7.655	3.166	6.054	3.383	6.346	3.008
ISO Sm	171.367	127.429	157.967	16 0.580	148.931	158.375	246.444	129.184	174.815	149.988	162.508	33.331
ISO Wt	164.993	83.598	48.742	73.812	36.314	61.191	72.529	26.238	69.533	38.302	67.525	39.091
ISO Rmax	124.919	64.148	40.226	39.751	12.510	53.490	45.010	20.743	61.622	33.138	49.556	31.144
ISO Rv	83.147	73.784	34.931	53.168	28.233	47.918	54.832	16.857	52.918	27.394	47.318	20.947
ISO Rz	73.292	34.047	24.477	38.971	15.972	32.127	36.255	16.943	26.480	19.270	31.783	16.694

Surface Topography

Group 2 icon-saliva 30 days

		a	b	c	Ave
1	ISO Am	66.588	70.938	64.900	67.475
	ISO Ra	7.700	7.638	8.047	7.795
	ISO Sm	107.064	138.289	157.025	134.126
	ISO Wt	82.831	84.463	84.050	83.781
	ISO Rmax	82.101	68.282	64.853	71.745
	ISO Rv	66.588	70.938	64.900	67.475
	ISO Rz	42.241	40.940	39.880	41.020

		a	b	c	Ave
2	ISO Am	53.804	42.211	90.984	62.333
	ISO Ra	7.878	7.362	10.040	8.427
	ISO Sm	152.765	109.469	134.431	132.222
	ISO Wt	72.211	57.812	123.725	84.583
	ISO Rmax	48.811	56.762	73.241	59.605
	ISO Rv	53.804	42.211	90.984	62.333
	ISO Rz	38.472	30.386	52.750	40.536

		a	b	c	Ave
3	ISO Am	73.021	47.907	35.795	52.241
	ISO Ra	7.098	6.149	6.011	6.419
	ISO Sm	78.907	115.216	107.935	100.686
	ISO Wt	123.348	63.133	53.646	80.042
	ISO Rmax	47.602	39.887	49.474	45.654
	ISO Rv	73.021	47.907	35.795	52.241
	ISO Rz	48.370	31.442	32.202	37.338

		a	b	c	Ave
4	ISO Am	98.984	115.251	98.553	104.263
	ISO Ra	12.950	12.265	12.620	12.612
	ISO Sm	117.194	107.305	93.348	105.949
	ISO Wt	176.267	199.326	192.775	189.456
	ISO Rmax	169.059	199.326	192.775	187.053
	ISO Rv	98.984	115.251	98.553	104.263
	ISO Rz	92.303	87.137	94.497	91.312

		a	b	c	Ave
5	ISO Am	32.576	99.551	86.622	72.916
	ISO Ra	7.887	9.940	9.759	9.195
	ISO Sm	91.779	83.351	103.609	92.913
	ISO Wt	60.022	208.758	133.104	133.961
	ISO Rmax	57.429	208.758	119.899	128.695
	ISO Rv	32.576	99.551	86.622	72.916
	ISO Rz	49.110	97.374	78.655	75.046

6	ISO Am	73.444	47.735	58.826	60.002
	ISO Ra	7.409	6.833	7.742	7.328
	ISO Sm	88.948	100.676	141.444	110.356
	ISO Wt	92.642	63.500	79.329	78.490
	ISO Rmax	89.147	56.879	65.397	70.474
	ISO Rv	73.444	47.735	58.826	60.002
	ISO Rz	45.216	33.831	41.508	40.185

7	ISO Am	106.330	131.090	168.429	135.283
	ISO Ra	9.728	10.200	6.472	8.800
	ISO Sm	121.092	81.811	106.656	103.186
	ISO Wt	127.278	164.553	189.058	160.296
	ISO Rmax	124.554	53.984	29.864	69.467
	ISO Rv	106.330	131.090	168.429	135.283
	ISO Rz	64.646	59.835	54.150	59.544

8	ISO Am	35.173	79.548	63.079	59.267
	ISO Ra	4.534	5.352	4.992	4.959
	ISO Sm	61.900	81.512	80.354	74.589
	ISO Wt	50.187	96.969	80.682	75.946
	ISO Rmax	37.462	89.775	74.795	67.344
	ISO Rv	35.173	79.548	63.079	59.267
	ISO Rz	29.480	40.337	36.128	35.315

9	ISO Am	107.481	76.106	72.533	85.373
	ISO Ra	7.825	7.686	8.906	8.139
	ISO Sm	106.551	75.309	100.936	94.265
	ISO Wt	143.747	170.234	339.594	217.858
	ISO Rmax	133.034	77.729	331.491	180.751
	ISO Rv	107.481	76.106	72.533	85.373
	ISO Rz	70.443	66.810	112.586	83.280

10	ISO Am	88.089	47.269	45.097	60.152
	ISO Ra	8.434	6.085	6.099	6.873
	ISO Sm	66.616	75.880	81.884	74.793
	ISO Wt	209.805	66.634	60.710	112.383
	ISO Rmax	209.805	59.511	56.638	108.651
	ISO Rv	88.089	47.269	45.097	60.152
	ISO Rz	77.837	44.158	40.981	54.325

Average Surface Topography

Group 2 icon-saliva 30 days

	1	2	3	4	5	6	7	8	9	10	Ave	STDEV
ISO Am	67.475	62.333	52.241	104.263	72.916	60.002	135.283	59.267	85.373	60.152	75.930	25.866
ISO Ra	7.795	8.427	6.419	12.612	9.195	7.328	8.800	4.959	8.139	6.873	8.055	2.028
ISO Sm	134.126	132.222	100.686	105.949	92.913	110.356	103.186	74.589	94.265	74.793	102.309	20.185
ISO Wt	83.781	84.583	80.042	189.456	133.961	78.490	160.296	75.946	217.858	112.383	121.680	51.721
ISO Rmax	71.745	59.605	45.654	187.053	128.695	70.474	69.467	67.344	180.751	108.651	98.944	50.816
ISO Rv	67.475	62.333	52.241	104.263	72.916	60.002	135.283	59.267	85.373	60.152	75.930	25.866
ISO Rz	41.020	40.536	37.338	91.312	75.046	40.185	59.544	35.315	83.280	54.325	55.790	20.706

Surface Topography

Group 3 MIP saliva baseline

		a	b	c	Ave
1	ISO Am	37.007	26.552	36.406	33.322
	ISO Ra	5.493	4.849	5.368	5.237
	ISO Sm	69.414	72.526	76.915	72.952
	ISO Wt	81.653	56.108	80.188	72.650
	ISO Rmax	74.834	56.108	68.941	66.628
	ISO Rv	37.007	26.552	36.406	33.322
	ISO Rz	41.182	32.591	37.090	36.954

2	ISO Am	31.108	26.34	21.488	26.312
	ISO Ra	6.087	5.771	5.360	5.739
	ISO Sm	80.959	102.978	80.935	88.291
	ISO Wt	52.61	146.228	37.786	78.875
	ISO Rmax	44.132	139.477	34.177	72.595
	ISO Rv	31.108	26.34	21.488	26.312
	ISO Rz	36.19	56.555	28.591	40.445

3	ISO Am	39.535	48.381	41.991	43.302
	ISO Ra	6.157	6.478	6.062	6.232
	ISO Sm	68.101	71.664	74.239	71.335
	ISO Wt	172.432	179.432	149.967	167.277
	ISO Rmax	156.15	147.823	131.456	145.143
	ISO Rv	39.535	48.381	41.991	43.302
	ISO Rz	63.56	62.785	56.589	60.978

4	ISO Am	29.792	34.252	41.229	35.091
	ISO Ra	5.786	5.78	5.006	5.524
	ISO Sm	71.964	68.543	63.241	67.916
	ISO Wt	61.847	71.145	74.725	69.239
	ISO Rmax	61.847	71.145	68.150	67.047
	ISO Rv	29.792	34.252	41.229	35.091
	ISO Rz	43.909	44.78	38.853	42.514

5	ISO Am	30.562	37.206	38.337	35.368
	ISO Ra	4.717	6.764	7.051	6.177
	ISO Sm	106.56	99.275	127.829	111.221
	ISO Wt	106.036	114.549	94.343	104.976
	ISO Rmax	84.279	90.361	68.030	80.890
	ISO Rv	30.562	37.206	38.337	35.368
	ISO Rz	37.068	53.283	45.389	45.247

6	ISO Am	59.872	58.056	51.697	56.542
	ISO Ra	7.266	7.057	7.179	7.167
	ISO Sm	92.559	112.847	95.647	100.351
	ISO Wt	124.984	141.29	149.532	138.602
	ISO Rmax	124.984	141.29	149.532	138.602
	ISO Rv	59.872	58.056	51.697	56.542
	ISO Rz	54.868	53.41	55.431	54.570

7	ISO Am	53.819	57.921	69.119	60.286
	ISO Ra	7.44	7.901	8.612	7.984
	ISO Sm	81.721	97.451	81.650	86.941
	ISO Wt	108.204	115.776	139.776	121.252
	ISO Rmax	108.204	115.776	139.776	121.252
	ISO Rv	53.819	57.921	69.119	60.286
	ISO Rz	50.326	55.69	62.293	56.103

8	ISO Am	44.017	42.61	44.471	43.699
	ISO Ra	5.749	5.409	5.895	5.684
	ISO Sm	83.423	88.2	88.712	86.778
	ISO Wt	88.735	63.112	89.352	80.400
	ISO Rmax	88.735	54.256	89.352	77.448
	ISO Rv	44.017	42.61	44.471	43.699
	ISO Rz	42.642	31.885	42.178	38.902

9	ISO Am	44.898	39.066	51.247	45.070
	ISO Ra	4.956	6.259	6.579	5.931
	ISO Sm	121.859	109.575	153.242	128.225
	ISO Wt	138.104	133.827	148.292	140.074
	ISO Rmax	116.76	114.139	121.437	117.445
	ISO Rv	44.898	39.066	51.247	45.070
	ISO Rz	45.382	47.449	50.935	47.922

10	ISO Am	57.971	50.327	70.067	59.455
	ISO Ra	6.293	6.042	5.679	6.005
	ISO Sm	65.062	69.828	62.003	65.631
	ISO Wt	112.497	96.883	128.495	112.625
	ISO Rmax	112.497	96.883	128.495	112.625
	ISO Rv	57.971	50.327	70.067	59.455
	ISO Rz	49.545	47.454	46.887	47.962

Average Surface Topography

Group 3 MIP saliva baseline

	1	2	3	4	5	6	7	8	9	10	Ave	STDEV
ISO Am	33.322	26.312	43.302	35.091	35.368	56.542	60.286	43.699	45.070	59.455	43.845	11.755
ISO Ra	5.237	5.739	6.232	5.524	6.177	7.167	7.984	5.684	5.931	6.005	6.168	0.822
ISO Sm	72.952	88.291	71.335	67.916	111.221	100.351	86.941	86.778	128.225	65.631	87.964	20.332
ISO Wt	72.650	78.875	167.277	69.239	104.976	138.602	121.252	80.400	140.074	112.625	108.597	33.406
ISO Rmax	66.628	72.595	145.143	67.047	80.890	138.602	121.252	77.448	117.445	112.625	99.968	30.309
ISO Rv	33.322	26.312	43.302	35.091	35.368	56.542	60.286	43.699	45.070	59.455	43.845	11.755
ISO Rz	36.954	40.445	60.978	42.514	45.247	54.570	56.103	38.902	47.922	47.962	47.160	7.956

Surface Topography

Group 3 MIP saliva demineralization

		a	b	c	Ave
1	ISO Am	24.773	31.246	38.102	31.374
	ISO Ra	4.031	4.196	4.361	4.196
	ISO Sm	133.076	142.139	129.982	135.066
	ISO Wt	43.165	51.415	48.131	47.570
	ISO Rmax	25.807	33.547	32.838	30.731
	ISO Rv	24.773	31.246	38.102	31.374
	ISO Rz	21.510	24.801	23.324	23.212
2	ISO Am	24.443	27.600	31.952	27.998
	ISO Ra	8.676	7.347	5.292	7.105
	ISO Sm	193.170	246.161	202.843	214.058
	ISO Wt	53.954	56.834	67.024	59.271
	ISO Rmax	48.919	40.737	59.616	49.757
	ISO Rv	24.443	27.600	31.952	27.998
	ISO Rz	36.488	33.504	38.524	36.172
3	ISO Am	39.523	35.571	37.854	37.649
	ISO Ra	5.655	6.386	5.676	5.906
	ISO Sm	99.533	111.267	98.893	103.231
	ISO Wt	56.585	55.589	54.476	55.550
	ISO Rmax	45.812	46.419	29.554	40.595
	ISO Rv	39.523	35.571	37.854	37.649
	ISO Rz	32.867	38.617	32.385	34.623
4	ISO Am	36.163	27.221	25.811	29.732
	ISO Ra	4.873	4.757	4.573	4.734
	ISO Sm	73.671	74.140	56.605	68.139
	ISO Wt	53.043	43.936	44.685	47.221
	ISO Rmax	49.022	41.747	37.273	42.681
	ISO Rv	36.163	27.221	25.811	29.732
	ISO Rz	32.717	29.125	28.441	30.094
5	ISO Am	32.968	26.124	24.816	27.969
	ISO Ra	4.897	5.700	5.407	5.335
	ISO Sm	157.278	498.414	388.430	348.041
	ISO Wt	51.525	49.700	38.565	46.597
	ISO Rmax	34.058	39.950	33.594	35.867
	ISO Rv	32.968	26.124	24.816	27.969
	ISO Rz	25.226	26.512	25.342	25.693

6	ISO Am	59.376	49.346	52.358	53.693
	ISO Ra	6.829	6.609	6.926	6.788
	ISO Sm	243.646	168.049	126.935	179.543
	ISO Wt	81.851	69.874	65.666	72.464
	ISO Rmax	72.877	59.991	60.656	64.508
	ISO Rv	59.376	49.346	52.358	53.693
	ISO Rz	39.195	34.973	33.923	36.030

7	ISO Am	48.119	49.373	53.710	50.401
	ISO Ra	4.899	5.792	5.680	5.457
	ISO Sm	184.479	299.649	320.039	268.056
	ISO Wt	97.270	61.721	64.217	74.403
	ISO Rmax	97.270	60.932	64.217	74.140
	ISO Rv	48.119	49.373	53.710	50.401
	ISO Rz	34.755	29.363	28.524	30.881

8	ISO Am	57.675	49.020	44.383	50.359
	ISO Ra	5.496	5.509	5.198	5.401
	ISO Sm	92.953	88.061	91.825	90.946
	ISO Wt	72.291	63.217	63.533	66.347
	ISO Rmax	71.442	59.716	58.833	63.330
	ISO Rv	57.675	49.020	44.383	50.359
	ISO Rz	32.428	32.117	35.283	33.276

9	ISO Am	40.852	64.738	37.416	47.669
	ISO Ra	5.048	5.596	6.751	5.798
	ISO Sm	161.018	127.456	117.748	135.407
	ISO Wt	56.547	161.209	61.066	92.941
	ISO Rmax	25.423	118.453	48.755	64.210
	ISO Rv	40.852	64.738	37.416	47.669
	ISO Rz	28.910	50.743	39.949	39.867

10	ISO Am	48.875	45.053	49.870	47.933
	ISO Ra	5.099	5.232	4.944	5.092
	ISO Sm	81.047	102.754	93.377	92.393
	ISO Wt	69.631	63.752	67.547	66.977
	ISO Rmax	60.278	56.891	60.665	59.278
	ISO Rv	48.875	45.053	49.870	47.933
	ISO Rz	30.906	32.023	30.938	31.289

Average Surface Topography

Group 3 MIP saliva demineralization

	1	2	3	4	5	6	7	8	9	10	Ave	STDEV
ISO Am	31.374	27.998	37.649	29.732	27.969	53.693	50.401	50.359	47.669	47.933	40.478	10.523
ISO Ra	4.196	7.105	5.906	4.734	5.335	6.788	5.457	5.401	5.798	5.092	5.581	0.877
ISO Sm	135.07	214.06	103.23	68.139	348.04	179.54	268.06	90.946	135.4	92.393	163.5	89.719
ISO Wt	47.570	59.271	55.550	47.221	46.597	72.464	74.403	66.347	92.941	66.977	62.934	14.789
ISO Rmax	30.731	49.757	40.595	42.681	35.867	64.508	74.140	63.330	64.210	59.278	52.510	14.564
ISO Rv	31.374	27.998	37.649	29.732	27.969	53.693	50.401	50.359	47.669	47.933	40.478	10.523
ISO Rz	23.212	36.172	34.623	30.094	25.693	36.030	30.881	33.276	39.867	31.289	32.114	5.015

Surface Topography

Group 3 MIP saliva 30 days

E1A				Ave
Am	24.266	28.654	35.649	29.523
Ra	4.163	4.736	4.628	4.509
Sm	87.281	78.18	116.275	93.912
Wt	62.66	72.306	84.045	73.003667
Rmax	62.66	66.717	75.166	68.181
Rv	24.266	28.654	35.649	29.523
Rz	31.164	36.976	35.64	34.593333

E2A				Ave
Am	26.545	20.56	24.019	23.708
Ra	6.487	6.298	4.708	5.831
Sm	198.783	271.172	109.236	193.06367
Wt	150.715	138.658	141.655	143.676
Rmax	133.537	135.466	123.604	130.869
Rv	26.545	20.56	24.019	23.708
Rz	53.458	48.494	47.515	49.822333

E3A				Ave
Am	34.353	44.433	33.06	37.282
Ra	6.011	7.441	5.311	6.2543333
Sm	101.892	118.976	81.215	100.69433
Wt	150.994	150.001	132.256	144.417
Rmax	140.951	133.433	121.176	131.85333
Rv	34.353	44.433	33.06	37.282
Rz	56.246	63.689	49.107	56.347333

E4A				Ave
Am	36.96	28.902	33.095	32.985667
Ra	4.547	4.908	4.923	4.7926667
Sm	93.233	62.145	69.874	75.084
Wt	74.71	58.505	63.719	65.644667
Rmax	74.71	58.505	63.719	65.644667
Rv	36.96	28.902	33.095	32.985667
Rz	30.908	33.614	32.68	32.400667

E5A				Ave
Am	54.918	49.451	47.168	50.512333
Ra	4.923	5.834	6.343	5.7
Sm	395.177	277.084	293.281	321.84733
Wt	65.784	204.431	60.774	110.32967
Rmax	23.795	163.285	31.386	72.822
Rv	54.918	49.451	47.168	50.512333
Rz	25.204	55.23	28.086	36.173333

E6A				Ave
Am	55.614	49.725	51.855	52.398
Ra	6.943	6.836	7.042	6.9403333
Sm	117.191	139.041	148.426	134.886
Wt	137.394	63.734	155.79	118.97267
Rmax	137.394	54.172	151.48	114.34867
Rv	55.614	49.725	51.855	52.398
Rz	49.044	33.667	52.654	45.121667

E7A				Ave
Am	49.11	56.081	55.134	53.441667
Ra	5.263	5.415	5.553	5.4103333
Sm	197.901	167.582	177.595	181.026
Wt	63.846	76.94	111.041	83.942333
Rmax	59.214	76.94	111.041	82.398333
Rv	49.11	56.081	55.134	53.441667
Rz	29.316	33.468	40.596	34.46

E8A				Ave
Am	62.226	57.257	49.09	56.191
Ra	5.405	5.338	5.204	5.3156667
Sm	86.932	99.545	89.23	91.902333
Wt	124.718	114.737	98.717	112.724
Rmax	124.718	114.737	98.717	112.724
Rv	62.226	57.257	49.09	56.191
Rz	41.646	40.972	38.705	40.441

E9A				Ave
Am	57.281	68.669	66.805	64.251667
Ra	6.895	6.831	7.812	7.1793333
Sm	107.043	214.626	186.107	169.25867
Wt	190.013	228.293	255.389	224.565
Rmax	165.521	184.65	233.672	194.61433
Rv	57.281	68.669	66.805	64.251667
Rz	68.865	67.208	76.445	70.839333

E10A				Ave
Am	43.303	45.867	49.694	46.288
Ra	4.952	4.84	4.595	4.7956667
Sm	73.984	81.169	122.938	92.697
Wt	87.145	91.693	61.747	80.195
Rmax	87.145	91.693	61.588	80.142
Rv	43.303	45.867	49.694	46.288
Rz	45.154	45.895	29.054	40.034333

Average Surface Topography

Group 3 MIP saliva 30 days

	1	2	3	4	5	6	7	8	9	10	Ave	STDEV
ISO Am	29.52	23.70	37.282	32.98	50.512	52.398	53.442	56.191	64.252	46.28	44.658	13.12
ISO Ra	4.509	5.831	6.254	4.793	5.700	6.940	5.410	5.316	7.179	4.796	5.673	0.903
ISO Sm	93.91	193.0	100.69	75.08	321.84	134.88	181.02	91.902	169.25	92.69	145.43	74.97
ISO Wt	73.00	143.6	144.41	65.645	110.330	118.973	83.942	112.724	224.565	80.195	115.747	47.264
ISO Rmax	68.18	130.8	131.85	65.645	72.822	114.349	82.398	112.724	194.614	80.142	105.360	40.326
ISO Rv	29.52	23.70	37.282	32.986	50.512	52.398	53.442	56.191	64.252	46.288	44.658	13.121
ISO Rz	34.59	49.82	56.347	32.401	36.173	45.122	34.460	40.441	70.839	40.034	44.023	12.072

Surface Topography

Group 4 icon water baseline

		a	b	c	Ave
1	ISO Am	43.46	36.914	41.248	40.541
	ISO Ra	6.438	4.482	4.601	5.174
	ISO Sm	99.89	154.35	121.236	125.159
	ISO Wt	72.564	74.724	82.783	76.690
	ISO Rmax	66.512	74.724	82.783	74.673
	ISO Rv	43.46	36.914	41.248	40.541
	ISO Rz	47.392	29.496	34.943	37.277

2	ISO Am	48.085	39.229	34.168	40.494
	ISO Ra	7.687	5.106	5.721	6.171
	ISO Sm	81.818	64.829	58.764	68.470
	ISO Wt	85.817	61.378	106.156	84.450
	ISO Rmax	85.817	34.819	104.433	75.023
	ISO Rv	48.085	39.229	34.168	40.494
	ISO Rz	54.051	38.616	55.642	49.436

3	ISO Am	30.368	50.769	22.205	34.447
	ISO Ra	5.431	15.236	4.869	8.512
	ISO Sm	139.506	361.817	89.928	197.084
	ISO Wt	60.842	92.401	49.183	67.475
	ISO Rmax	54.44	71.154	47.960	57.851
	ISO Rv	30.368	50.769	22.205	34.447
	ISO Rz	41.25	51.627	37.570	43.482

4	ISO Am	13.075	25.38	42.266	26.907
	ISO Ra	3.839	5.004	4.918	4.587
	ISO Sm	49.153	63.19	64.143	58.829
	ISO Wt	29.312	50.486	84.055	54.618
	ISO Rmax	26.783	45.195	84.055	52.011
	ISO Rv	13.075	25.38	42.266	26.907
	ISO Rz	24.142	35.561	42.166	33.956

5	ISO Am	51.502	51.548	53.613	52.221
	ISO Ra	6.363	5.879	6.716	6.319
	ISO Sm	98.378	98.464	109.369	102.070
	ISO Wt	77.375	73.98	205.115	118.823
	ISO Rmax	56.317	36.37	168.197	86.961
	ISO Rv	51.502	51.548	53.613	52.221
	ISO Rz	46.488	41.372	69.740	52.533

6	ISO Am	37.843	34.398	50.456	40.899
	ISO Ra	5.946	5.471	6.693	6.037
	ISO Sm	86.979	69.191	78.917	78.362
	ISO Wt	59.57	57.584	99.749	72.301
	ISO Rmax	58.277	55.929	99.749	71.318
	ISO Rv	37.843	34.398	50.456	40.899
	ISO Rz	39.997	41.829	53.989	45.272

7	ISO Am	51.027	34.543	39.997	41.856
	ISO Ra	5.828	5.891	5.829	5.849
	ISO Sm	63.81	67.519	58.310	63.213
	ISO Wt	82.02	68.137	80.088	76.748
	ISO Rmax	82.02	66.412	80.088	76.173
	ISO Rv	51.027	34.543	39.997	41.856
	ISO Rz	45.671	48.531	48.262	47.488

8	ISO Am	55.683	54.047	57.173	55.634
	ISO Ra	8.393	9.43	9.886	9.236
	ISO Sm	86.535	93.239	95.038	91.604
	ISO Wt	110.075	111.817	164.244	128.712
	ISO Rmax	91.81	87.992	148.592	109.465
	ISO Rv	55.683	54.047	57.173	55.634
	ISO Rz	63.568	62.995	79.118	68.560

9	ISO Am	33.09	33.314	36.372	34.259
	ISO Ra	4.549	5.031	5.066	4.882
	ISO Sm	74.718	83.583	93.628	83.976
	ISO Wt	50.75	52.889	72.711	58.783
	ISO Rmax	45.106	50.669	72.711	56.162
	ISO Rv	33.09	33.314	36.372	34.259
	ISO Rz	35.432	34.69	38.670	36.264

10	ISO Am	41.745	34.786	41.936	39.489
	ISO Ra	5.586	5.14	5.147	5.291
	ISO Sm	134.473	172.333	148.347	151.718
	ISO Wt	65.703	49.498	84.899	66.700
	ISO Rmax	62.385	48.139	84.899	65.141
	ISO Rv	41.745	34.786	41.936	39.489
	ISO Rz	41.175	33.122	43.025	39.107

Average Surface Topography

Group 4 icon water baseline

	1	2	3	4	5	6	7	8	9	10	Ave	STDEV
ISO Am	40.54	40.49	34.44	26.90	52.22	40.90	41.86	55.63	34.25	39.49	40.68	8.36
ISO Ra	5.17	6.17	8.51	4.59	6.32	6.01	5.85	9.24	4.88	5.29	6.21	1.53
ISO Sm	125.20	68.47	197.10	58.82	102.07	78.36	63.21	91.60	83.98	151.72	102.05	44.14
ISO Wt	76.69	84.45	67.47	54.61	118.23	72.30	76.75	128.71	58.78	66.70	80.53	24.51
ISO Rmax	74.67	75.02	57.85	52.01	86.961	71.32	76.17	109.47	56.16	65.14	72.48	16.86
ISO Rv	40.54	40.49	34.45	26.91	52.221	40.90	41.86	55.634	34.26	39.49	40.68	8.36
ISO Rz	37.28	49.43	43.48	33.96	52.533	45.27	47.49	68.560	36.26	39.11	45.34	10.17

Surface Topography

Group 4 icon water demineralization

		a	b	c	Ave
1	ISO Am	42.431	37.149	40.243	39.941
	ISO Ra	5.439	4.521	4.655	4.872
	ISO Sm	156.371	340.385	317.061	271.272
	ISO Wt	63.761	74.736	48.86	62.452
	ISO Rmax	63.761	74.736	47.869	62.122
	ISO Rv	42.431	37.149	40.243	39.941
	ISO Rz	37.88	29.687	23.426	30.331

2	ISO Am	41.114	32.33	28.29	33.911
	ISO Ra	6.338	3.786	3.833	4.652
	ISO Sm	203.325	91.889	198.899	164.704
	ISO Wt	67.069	50.018	38.226	51.771
	ISO Rmax	67.069	30.882	29.221	42.391
	ISO Rv	41.114	32.33	28.29	33.911
	ISO Rz	38.958	29.641	20.408	29.669

3	ISO Am	13.115	13.121	11.592	12.609
	ISO Ra	2.373	3.454	3.356	3.061
	ISO Sm	131.014	129.827	172.104	144.315
	ISO Wt	24.792	30.686	33.157	29.545
	ISO Rmax	17.042	30.686	32.403	26.710
	ISO Rv	13.115	13.121	11.592	12.609
	ISO Rz	15.834	24.357	25.747	21.979

4	ISO Am	28.177	28.413	25.333	27.308
	ISO Ra	2.33	3.777	3.617	3.241
	ISO Sm	164.44	199.898	191.778	185.372
	ISO Wt	37.468	49.042	38.463	41.658
	ISO Rmax	37.468	49.042	32.506	39.672
	ISO Rv	28.177	28.413	25.333	27.308
	ISO Rz	16.919	25.495	20.223	20.879

5	ISO Am	41.775	43.586	44.373	43.245
	ISO Ra	5.656	5.183	5.073	5.304
	ISO Sm	175.689	551.055	479.329	402.024
	ISO Wt	64.928	56.542	60.111	60.527
	ISO Rmax	40.102	37.363	29.122	35.529
	ISO Rv	41.775	43.586	44.373	43.245
	ISO Rz	37.878	29.541	26.674	31.364

6					
	ISO Am	31.9	38.522	34.302	34.908
	ISO Ra	3.851	4.239	4.002	4.031
	ISO Sm	189.474	358.596	472.093	340.054
	ISO Wt	44.174	50.785	43.866	46.275
	ISO Rmax	41.939	47.264	42.268	43.824
	ISO Rv	31.9	38.522	34.302	34.908
	ISO Rz	21.767	24.093	21.03	22.297

7					
	ISO Am	30.578	26.572	24.774	27.308
	ISO Ra	3.875	3.784	4.212	3.957
	ISO Sm	144.487	160.237	246.375	183.700
	ISO Wt	55.844	48.554	46.962	50.453
	ISO Rmax	49.285	44.642	42.501	45.476
	ISO Rv	30.578	26.572	24.774	27.308
	ISO Rz	30.376	29.573	29.124	29.691

8						8				
	ISO Am	50.941	55.409	49.616	51.989		ISO Am	50.941	55.409	53.175
	ISO Ra	8.021	6.934	7.915	7.623		ISO Ra	8.021	6.934	7.4775
	ISO Sm	255.288	191.975	342.4	263.221		ISO Sm	255.288	191.975	223.6315
	ISO Wt	92.49	83.087	153.987	109.855		ISO Wt	92.49	83.087	87.7885
	ISO Rmax	62.453	70.124	148.867	93.815		ISO Rmax	62.453	70.124	66.2885
	ISO Rv	50.941	55.409	49.616	51.989		ISO Rv	50.941	55.409	53.175
	ISO Rz	48.914	46.196	59.853	51.654		ISO Rz	48.914	46.196	47.555

9					
	ISO Am	27.843	44.037	29.483	33.788
	ISO Ra	3.936	4.948	4.944	4.609
	ISO Sm	167.749	96.506	143.754	136.003
	ISO Wt	39.606	69.273	59.655	56.178
	ISO Rmax	36.26	69.273	59.655	55.063
	ISO Rv	27.843	44.037	29.483	33.788
	ISO Rz	25.14	39.681	41.42	35.414

10					
	ISO Am	38.552	37.679	36.631	37.621
	ISO Ra	4.998	5.804	6.385	5.729
	ISO Sm	156.447	146.01	148.244	150.234
	ISO Wt	51.196	64.422	69.948	61.855
	ISO Rmax	46.454	49.23	67.297	54.327
	ISO Rv	38.552	37.679	36.631	37.621
	ISO Rz	33.046	43.2	51.263	42.503

Average Surface Topography

Group 4 icon water demineralization

	1	2	3	4	5	6	7	8	9	10	Ave	STDEV
ISO Am	39.94	33.91	12.61	27.31	43.25	34.91	27.31	53.18	33.79	37.62	34.38	10.79
ISO Ra	4.87	4.65	3.06	3.241	5.30	4.03	3.96	7.48	4.61	5.729	4.69	1.29
ISO Sm	271.27	164.70	144.32	188.37	402.02	340.05	183.70	223.63	136.00	150.23	220.13	90.32
ISO Wt	62.45	51.77	29.55	41.66	60.53	46.28	50.45	87.79	56.18	61.86	54.85	15.43
ISO Rmax	62.12	42.39	26.71	39.67	35.53	43.82	45.48	66.29	55.06	54.33	47.14	12.25
ISO Rv	39.94	33.91	12.61	27.31	43.25	34.91	27.31	53.18	33.79	37.62	34.38	10.79
ISO Rz	30.33	29.67	21.98	20.88	31.36	22.28	29.69	47.56	35.41	42.50	31.17	8.75

Surface Topography

Group 4 icon water 30 days

		a	b	c	Ave
1	ISO Am	49.942	57.788	59.306	55.679
	ISO Ra	5.83	5.392	5.493	5.572
	ISO Sm	104.291	107.799	70.503	94.198
	ISO Wt	76.973	111.474	116.515	101.654
	ISO Rmax	76.973	111.474	116.515	101.654
	ISO Rv	49.942	57.788	59.306	55.679
	ISO Rz	48.273	42.339	44.506	45.039

		a	b	c	Ave
2	ISO Am	74.16	115.817	106.594	98.857
	ISO Ra	6.868	8.93	18.657	11.485
	ISO Sm	58.351	59.381	88.166	68.633
	ISO Wt	112.609	157.497	206.009	158.705
	ISO Rmax	112.609	41.496	206.009	120.038
	ISO Rv	74.16	115.817	106.594	98.857
	ISO Rz	49.627	57.591	134.671	80.630

		a	b	c	Ave
3	ISO Am	26.67	33.685	33.249	31.201
	ISO Ra	3.818	4.672	6.264	4.918
	ISO Sm	76.435	112.944	183.202	124.194
	ISO Wt	62.693	67.598	67.286	65.859
	ISO Rmax	54.95	67.598	67.286	63.278
	ISO Rv	26.67	33.685	33.249	31.201
	ISO Rz	28.369	31.863	38.679	32.970

		a	b	c	Ave
4	ISO Am	42.443	41.773	65.868	50.028
	ISO Ra	6.284	5.52	6.987	6.264
	ISO Sm	78.961	61.71	63.74	68.137
	ISO Wt	70.878	72.081	93.175	78.711
	ISO Rmax	67.394	59.251	89.161	71.935
	ISO Rv	42.443	41.773	65.868	50.028
	ISO Rz	49.257	44.306	52.2	48.588

		a	b	c	Ave
5	ISO Am	82.662	122.908	119.281	108.284
	ISO Ra	8.651	7.364	8.452	8.156
	ISO Sm	97.45	85.269	70.551	84.423
	ISO Wt	176.075	144.113	147.544	155.911
	ISO Rmax	59	51.73	89.458	66.729
	ISO Rv	82.662	122.908	119.281	108.284
	ISO Rz	63.522	51.553	62.92	59.332

6	ISO Am	138.349	135.283	133.408	135.680
	ISO Ra	13.977	14.409	14.381	14.256
	ISO Sm	133.288	106.904	121.659	120.617
	ISO Wt	203.744	187.493	214.143	201.793
	ISO Rmax	186.584	182.328	214.143	194.352
	ISO Rv	138.349	135.283	133.408	135.680
	ISO Rz	91.921	84.84	97.198	91.320

7	ISO Am	35.449	44.021	69.542	49.671
	ISO Ra	4.559	6.007	5.577	5.381
	ISO Sm	51.974	67.966	64.495	61.478
	ISO Wt	68.288	77.488	107.608	84.461
	ISO Rmax	68.288	67.453	84.348	73.363
	ISO Rv	35.449	44.021	69.542	49.671
	ISO Rz	34.497	42.479	50.572	42.516

8	ISO Am	76.297	89.432	81.378	82.369
	ISO Ra	8.204	15.261	10.057	11.174
	ISO Sm	67.159	89.33	83.763	80.084
	ISO Wt	153.343	170.033	191.132	171.503
	ISO Rmax	110.249	135.604	135.925	127.259
	ISO Rv	76.297	89.432	81.378	82.369
	ISO Rz	70.897	104.573	99.989	91.820

9	ISO Am	46.327	93.422	67.526	69.092
	ISO Ra	5.637	7.483	6.152	6.424
	ISO Sm	62.966	57.856	68.115	62.979
	ISO Wt	69.33	202.269	89.128	120.242
	ISO Rmax	49.419	202.269	48.015	99.901
	ISO Rv	46.327	93.422	67.526	69.092
	ISO Rz	39.139	69.486	42.121	50.249

10	ISO Am	32.439	50.727	42.957	42.041
	ISO Ra	6.988	7.138	7.863	7.330
	ISO Sm	116.942	149.092	138.354	134.796
	ISO Wt	63.652	86.993	86.986	79.210
	ISO Rmax	61.689	72.18	86.986	73.618
	ISO Rv	32.439	50.727	42.957	42.041
	ISO Rz	42.782	48.029	55.679	48.830

Average Surface Topography

Group 4 icon water 30 days

	1	2	3	4	5	6	7	8	9	10	Ave	STDEV
ISO Am	55.679	98.857	31.2	50.03	108.280	135.680	49.67	82.37	69.092	42.04	72.290	33.363
ISO Ra	5.572	11.485	4.918	6.26	8.160	14.260	5.38	11.17	6.424	7.33	8.096	3.154
ISO Sm	94.198	68.633	124.2	68.14	84.420	120.620	61.48	80.08	62.979	134.8	89.955	27.365
ISO Wt	101.654	158.705	65.86	78.71	155.910	201.790	84.46	171.5	120.240	79.21	121.804	47.136
ISO Rmax	101.654	120.038	63.28	71.94	66.730	194.350	73.36	127.3	99.900	73.62	99.213	40.403
ISO Rv	55.679	98.857	31.2	50.03	108.280	135.680	49.67	82.37	69.090	42.04	72.290	33.363
ISO Rz	45.039	80.630	32.97	48.59	59.330	91.320	42.52	91.82	50.250	48.83	59.130	21.140

Surface Topography

Group 5 MIP humidity baseline

		a	b	c	Ave
1	ISO Am	37.007	26.552	36.406	33.322
	ISO Ra	5.493	4.849	5.368	5.237
	ISO Sm	69.414	72.526	76.915	72.952
	ISO Wt	81.653	56.108	80.188	72.650
	ISO Rmax	74.834	56.108	68.941	66.628
	ISO Rv	37.007	26.552	36.406	33.322
	ISO Rz	41.182	32.591	37.090	36.954

		a	b	c	Ave
2	ISO Am	31.108	26.34	21.488	26.312
	ISO Ra	6.087	5.771	5.360	5.739
	ISO Sm	80.959	102.978	80.935	88.291
	ISO Wt	52.61	146.228	37.786	78.875
	ISO Rmax	44.132	139.477	34.177	72.595
	ISO Rv	31.108	26.34	21.488	26.312
	ISO Rz	36.19	56.555	28.591	40.445

		a	b	c	Ave
3	ISO Am	39.535	48.381	41.991	43.302
	ISO Ra	6.157	6.478	6.062	6.232
	ISO Sm	68.101	71.664	74.239	71.335
	ISO Wt	172.432	179.432	149.967	167.277
	ISO Rmax	156.15	147.823	131.456	145.143
	ISO Rv	39.535	48.381	41.991	43.302
	ISO Rz	63.56	62.785	56.589	60.978

		a	b	c	Ave
4	ISO Am	29.792	34.252	41.229	35.091
	ISO Ra	5.786	5.78	5.006	5.524
	ISO Sm	71.964	68.543	63.241	67.916
	ISO Wt	61.847	71.145	74.725	69.239
	ISO Rmax	61.847	71.145	68.150	67.047
	ISO Rv	29.792	34.252	41.229	35.091
	ISO Rz	43.909	44.78	38.853	42.514

		a	b	c	Ave
5	ISO Am	30.562	37.206	38.337	35.368
	ISO Ra	4.717	6.764	7.051	6.177
	ISO Sm	106.56	99.275	127.829	111.221
	ISO Wt	106.036	114.549	94.343	104.976
	ISO Rmax	84.279	90.361	68.030	80.890
	ISO Rv	30.562	37.206	38.337	35.368
	ISO Rz	37.068	53.283	45.389	45.247

6	ISO Am	59.872	58.056	51.697	56.542
	ISO Ra	7.266	7.057	7.179	7.167
	ISO Sm	92.559	112.847	95.647	100.351
	ISO Wt	124.984	141.29	149.532	138.602
	ISO Rmax	124.984	141.29	149.532	138.602
	ISO Rv	59.872	58.056	51.697	56.542
	ISO Rz	54.868	53.41	55.431	54.570

7	ISO Am	53.819	57.921	69.119	60.286
	ISO Ra	7.44	7.901	8.612	7.984
	ISO Sm	81.721	97.451	81.650	86.941
	ISO Wt	108.204	115.776	139.776	121.252
	ISO Rmax	108.204	115.776	139.776	121.252
	ISO Rv	53.819	57.921	69.119	60.286
	ISO Rz	50.326	55.69	62.293	56.103

8	ISO Am	44.017	42.61	44.471	43.699
	ISO Ra	5.749	5.409	5.895	5.684
	ISO Sm	83.423	88.2	88.712	86.778
	ISO Wt	88.735	63.112	89.352	80.400
	ISO Rmax	88.735	54.256	89.352	77.448
	ISO Rv	44.017	42.61	44.471	43.699
	ISO Rz	42.642	31.885	42.178	38.902

9	ISO Am	44.898	39.066	51.247	45.070
	ISO Ra	4.956	6.259	6.579	5.931
	ISO Sm	121.859	109.575	153.242	128.225
	ISO Wt	138.104	133.827	148.292	140.074
	ISO Rmax	116.76	114.139	121.437	117.445
	ISO Rv	44.898	39.066	51.247	45.070
	ISO Rz	45.382	47.449	50.935	47.922

10	ISO Am	57.971	50.327	70.067	59.455
	ISO Ra	6.293	6.042	5.679	6.005
	ISO Sm	65.062	69.828	62.003	65.631
	ISO Wt	112.497	96.883	128.495	112.625
	ISO Rmax	112.497	96.883	128.495	112.625
	ISO Rv	57.971	50.327	70.067	59.455
	ISO Rz	49.545	47.454	46.887	47.962

Average Surface Topography

Group 5 MIP humidity baseline

	1	2	3	4	5	6	7	8	9	10	Ave	STDEV
ISO Am	33.32	26.31	43.302	35.091	35.368	56.542	60.286	43.699	45.070	59.455	43.845	11.755
ISO Ra	5.237	5.739	6.232	5.524	6.177	7.167	7.984	5.684	5.931	6.005	6.168	0.822
ISO Sm	72.95	88.29	71.335	67.916	111.22	100.35	86.941	86.778	128.23	65.631	87.964	20.333
ISO Wt	72.65	78.86	167.28	69.239	104.98	138.60	80.40	80.400	140.07	112.63	99.98	33.406
ISO Rmax	66.63	72.60	145.14	67.047	80.890	138.60	77.45	77.448	117.45	112.62	99.967	30.308
ISO Rv	33.32	26.31	43.302	35.091	35.368	56.540	60.290	43.699	45.070	59.455	43.845	11.755
ISO Rz	36.95	40.45	60.980	42.514	45.247	54.570	56.103	38.902	47.922	47.962	47.160	7.957

Surface Topography

Group 5 MIP humidity demineralization

		a	b	c	Ave
1	ISO Am	24.773	31.246	38.102	31.374
	ISO Ra	4.031	4.196	4.361	4.196
	ISO Sm	133.076	142.139	129.982	135.066
	ISO Wt	43.165	51.415	48.131	47.570
	ISO Rmax	25.807	33.547	32.838	30.731
	ISO Rv	24.773	31.246	38.102	31.374
	ISO Rz	21.510	24.801	23.324	23.212

		a	b	c	Ave
2	ISO Am	24.443	27.600	31.952	27.998
	ISO Ra	8.676	7.347	5.292	7.105
	ISO Sm	193.170	246.161	202.843	214.058
	ISO Wt	53.954	56.834	67.024	59.271
	ISO Rmax	48.919	40.737	59.616	49.757
	ISO Rv	24.443	27.600	31.952	27.998
	ISO Rz	36.488	33.504	38.524	36.172

		a	b	c	Ave
3	ISO Am	39.523	35.571	37.854	37.649
	ISO Ra	5.655	6.386	5.676	5.906
	ISO Sm	99.533	111.267	98.893	103.231
	ISO Wt	56.585	55.589	54.476	55.550
	ISO Rmax	45.812	46.419	29.554	40.595
	ISO Rv	39.523	35.571	37.854	37.649
	ISO Rz	32.867	38.617	32.385	34.623

		a	b	c	Ave
4	ISO Am	36.163	27.221	25.811	29.732
	ISO Ra	4.873	4.757	4.573	4.734
	ISO Sm	73.671	74.140	56.605	68.139
	ISO Wt	53.043	43.936	44.685	47.221
	ISO Rmax	49.022	41.747	37.273	42.681
	ISO Rv	36.163	27.221	25.811	29.732
	ISO Rz	32.717	29.125	28.441	30.094

		a	b	c	Ave
5	ISO Am	32.968	26.124	24.816	27.969
	ISO Ra	4.897	5.700	5.407	5.335
	ISO Sm	157.278	498.414	388.430	348.041
	ISO Wt	51.525	49.700	38.565	46.597
	ISO Rmax	34.058	39.950	33.594	35.867
	ISO Rv	32.968	26.124	24.816	27.969
	ISO Rz	25.226	26.512	25.342	25.693

6	ISO Am	59.376	49.346	52.358	53.693
	ISO Ra	6.829	6.609	6.926	6.788
	ISO Sm	243.646	168.049	126.935	179.543
	ISO Wt	81.851	69.874	65.666	72.464
	ISO Rmax	72.877	59.991	60.656	64.508
	ISO Rv	59.376	49.346	52.358	53.693
	ISO Rz	39.195	34.973	33.923	36.030

7	ISO Am	48.119	49.373	53.710	50.401
	ISO Ra	4.899	5.792	5.680	5.457
	ISO Sm	184.479	299.649	320.039	268.056
	ISO Wt	97.270	61.721	64.217	74.403
	ISO Rmax	97.270	60.932	64.217	74.140
	ISO Rv	48.119	49.373	53.710	50.401
	ISO Rz	34.755	29.363	28.524	30.881

8	ISO Am	57.675	49.020	44.383	50.359
	ISO Ra	5.496	5.509	5.198	5.401
	ISO Sm	92.953	88.061	91.825	90.946
	ISO Wt	72.291	63.217	63.533	66.347
	ISO Rmax	71.442	59.716	58.833	63.330
	ISO Rv	57.675	49.020	44.383	50.359
	ISO Rz	32.428	32.117	35.283	33.276

9	ISO Am	40.852	64.738	37.416	47.669
	ISO Ra	5.048	5.596	6.751	5.798
	ISO Sm	161.018	127.456	117.748	135.407
	ISO Wt	56.547	161.209	61.066	92.941
	ISO Rmax	25.423	118.453	48.755	64.210
	ISO Rv	40.852	64.738	37.416	47.669
	ISO Rz	28.910	50.743	39.949	39.867

10	ISO Am	48.875	45.053	49.870	47.933
	ISO Ra	5.099	5.232	4.944	5.092
	ISO Sm	81.047	102.754	93.377	92.393
	ISO Wt	69.631	63.752	67.547	66.977
	ISO Rmax	60.278	56.891	60.665	59.278
	ISO Rv	48.875	45.053	49.870	47.933
	ISO Rz	30.906	32.023	30.938	31.289

Average Surface Topography

Group 5 MIP humidity demineralization

	1	2	3	4	5	6	7	8	9	10	Ave	STDEV
ISO Am	31.374	27.998	37.649	29.732	27.969	53.693	50.401	50.359	47.669	47.933	40.478	10.523
ISO Ra	4.196	7.105	5.906	4.734	5.335	6.788	5.457	5.401	5.798	5.092	5.581	0.877
ISO Sm	135.066	214.058	103.231	68.139	348.041	179.543	268.056	90.946	135.407	92.393	163.488	89.719
ISO Wt	47.570	59.271	55.550	47.221	46.597	72.464	74.403	66.347	92.941	66.977	62.934	14.789
ISO Rmax	30.731	49.757	40.595	42.681	35.867	64.508	74.140	63.330	64.210	59.278	52.510	14.564
ISO Rv	31.374	27.998	37.649	29.732	27.969	53.693	50.401	50.359	47.669	47.933	40.478	10.523
ISO Rz	23.212	36.172	34.623	30.094	25.693	36.030	30.881	33.276	39.867	31.289	32.114	5.015

Surface Topography

Group 5 MIP humidity 30 days

E1A				Ave
Am	24.266	28.654	35.649	29.523
Ra	4.163	4.736	4.628	4.509
Sm	87.281	78.18	116.275	93.912
Wt	62.66	72.306	84.045	73.00367
Rmax	62.66	66.717	75.166	68.181
Rv	24.266	28.654	35.649	29.523
Rz	31.164	36.976	35.64	34.59333

E2A				Ave
Am	26.545	20.56	24.019	23.708
Ra	6.487	6.298	4.708	5.831
Sm	198.783	271.172	109.236	193.0637
Wt	150.715	138.658	141.655	143.676
Rmax	133.537	135.466	123.604	130.869
Rv	26.545	20.56	24.019	23.708
Rz	53.458	48.494	47.515	49.82233

E3A				Ave
Am	34.353	44.433	33.06	37.282
Ra	6.011	7.441	5.311	6.254333
Sm	101.892	118.976	81.215	100.6943
Wt	150.994	150.001	132.256	144.417
Rmax	140.951	133.433	121.176	131.8533
Rv	34.353	44.433	33.06	37.282
Rz	56.246	63.689	49.107	56.34733

E4A				Ave
Am	36.96	28.902	33.095	32.98567
Ra	4.547	4.908	4.923	4.792667
Sm	93.233	62.145	69.874	75.084
Wt	74.71	58.505	63.719	65.64467
Rmax	74.71	58.505	63.719	65.64467
Rv	36.96	28.902	33.095	32.98567
Rz	30.908	33.614	32.68	32.40067

E5A				Ave
Am	54.918	49.451	47.168	50.51233
Ra	4.923	5.834	6.343	5.7
Sm	395.177	277.084	293.281	321.8473
Wt	65.784	204.431	60.774	110.3297
Rmax	23.795	163.285	31.386	72.822
Rv	54.918	49.451	47.168	50.51233
Rz	25.204	55.23	28.086	36.17333

E6A				Ave
Am	55.614	49.725	51.855	52.398
Ra	6.943	6.836	7.042	6.940333
Sm	117.191	139.041	148.426	134.886
Wt	137.394	63.734	155.79	118.9727
Rmax	137.394	54.172	151.48	114.3487
Rv	55.614	49.725	51.855	52.398
Rz	49.044	33.667	52.654	45.12167

E7A				Ave
Am	49.11	56.081	55.134	53.44167
Ra	5.263	5.415	5.553	5.410333
Sm	197.901	167.582	177.595	181.026
Wt	63.846	76.94	111.041	83.94233
Rmax	59.214	76.94	111.041	82.39833
Rv	49.11	56.081	55.134	53.44167
Rz	29.316	33.468	40.596	34.46

E8A				Ave
Am	62.226	57.257	49.09	56.191
Ra	5.405	5.338	5.204	5.315667
Sm	86.932	99.545	89.23	91.90233
Wt	124.718	114.737	98.717	112.724
Rmax	124.718	114.737	98.717	112.724
Rv	62.226	57.257	49.09	56.191
Rz	41.646	40.972	38.705	40.441

E9A				Ave
Am	57.281	68.669	66.805	64.25167
Ra	6.895	6.831	7.812	7.179333
Sm	107.043	214.626	186.107	169.2587
Wt	190.013	228.293	255.389	224.565
Rmax	165.521	184.65	233.672	194.6143
Rv	57.281	68.669	66.805	64.25167
Rz	68.865	67.208	76.445	70.83933

E10A				Ave
Am	43.303	45.867	49.694	46.288
Ra	4.952	4.84	4.595	4.795667
Sm	73.984	81.169	122.938	92.697
Wt	87.145	91.693	61.747	80.195
Rmax	87.145	91.693	61.588	80.142
Rv	43.303	45.867	49.694	46.288
Rz	45.154	45.895	29.054	40.03433

Average Surface Topography

Group 5 MIP humidity 30 days

	1	2	3	4	5	6	7	8	9	10	Ave	STDEV
ISO Am	29.523	23.708	37.282	32.986	50.512	52.398	53.442	56.191	64.252	46.288	44.658	13.121
ISO Ra	4.509	5.831	6.254	4.793	5.700	6.940	5.410	5.316	7.179	4.796	5.673	0.903
ISO Sm	93.912	193.064	100.694	75.084	321.847	134.886	181.026	91.902	169.259	92.697	145.437	74.973
ISO Wt	73.004	143.676	144.417	65.645	110.330	118.973	83.942	112.724	224.565	80.195	115.747	47.264
ISO Rmax	68.181	130.869	131.853	65.645	72.822	114.349	82.398	112.724	194.614	80.142	105.360	40.326
ISO Rv	29.523	23.708	37.282	32.986	50.512	52.398	53.442	56.191	64.252	46.288	44.658	13.121
ISO Rz	34.593	49.822	56.347	32.401	36.173	45.122	34.460	40.441	70.839	40.034	44.023	12.072

Literature Cited

Ardu S, Castioni NV, Benbachir N, Krejci I. Minimally invasive treatment of white spot enamel lesions. Quintessence Int 2007; 38(8): 633-6.

Berkowitz RJ, Koo H, McDermott MP, Whelehan MT, Ragusa P, Kopycka-Kedzierawski DT, Karp JM, Billings R. Adjunctive chemotherapeutic suppression of mutans streptococci in the setting of severe early childhood caries: an exploratory study. J Public Health Dent. 2009 Summer;69(3):163-7.

Burgess j, Cakir D. Surface roughness determination of a caries infiltrant resin. Data on file. DMG 2010; Hamburg, Germany.

Casals E, Boukpessi T, McQueen CM, Eversole SL, Faller RV. Anticaries potential of commercial dentifrices as determined by fluoridation and remineralization efficiency. J Contemp Dent Prac 2007; 8: 1-19.

Cochrane NJ, Saranathan S, Cai F, Cross KJ, Reynolds EC. Enamel subsurface lesion remineralisation with casein phosphopeptide stabilised solutions of calcium, phosphate and fluoride. Caries Res 2008; 42: 88-97.

Croll TP Killian CM, Miller AS. Effect of enamel microabrasion compoud on human gingiva: report of a case. Quintessence Int 1990; 21: 959-63.

Croll TP, Cavanaugh RR. Enamel color modification by controlled hydrocloric acid pumice abrasion. I. Technique and examples. Quintessence Int 1986; 17: 81-7.

Curry JA, Tenuta LMA, Ribiero, CCC, Paes Leme AF. The importance of fluoride dentifrices to the current dental caries prevalence in Brazil. Braz Dent J 2004; 15: 167-74.

Donly KJ, Ruiz M. In vitro demineralization inhibition of enamel caries utilizing an unfilled resin. Clin Prev Dent 1992; 14: 22–24.

Du MQ, Tai BJ, Jiang H, Lo ECM, Fan MW, Bian Z. A two-year randomized clinical trial of chlorhexidine varnish on dental caries in Chinese preschool children. J Dent Res. 2006 Jun; 85(6): 557-9.

Ellwood R, Fejerskov O, Cury JA, Clarkson B. Fluoride in caries control. In: Fejerskov O, Kidd E, editors. Dental caries: the disease and its clinical management. 2nd ed. Oxford: Blackwell and Munksgaard; 2008; 287-323.

ElSayad I, Sakr A, Badr Y. Combining casein phosphopeptide-amorphous calcium phosphate with fluoride: synergistic remineralization potential of artificially demineralized enamel or not? J of Biomedical Optics 2009; 14: 044039.

Ericson D, Kidd E, McComb D, Mjör I, Noack MJ. Minimally Invasive Dentistry--concepts and techniques in cariology. Oral Health Prev Dent. 2003; 1: 59-72.

Featherstone JDB, Mellberg JR. Relative rates of progress of artificial carious lesions in bovine, ovine and human enamel. Caries Res 1981; 15: 109–114.

Featherstone JDB, Rodgers BE. The effect of acetic, lactic and other organic acids on the formation of artificial carious lesions. Caries Res 1981; 15: 377–385.

Featherstone JDB. Prevention and reversal of dental caries: role of low level fluoride. Community Dent Oral Epidemiol 1999; 27: 31–40.

Featherstone JD. The science and practice of caries prevention. Journal of American Dental Association 2000; 131: 887–99.

Featherstone JD. The continuum of dental caries—evidence for a dynamic disease process. Journal of Dental Research 2004; 83: C39–C42 [Spec Iss C].

Featherstone JD, Rapozo-Hilo ML, Rechmann P, Rechmann B, Greenspan D. In vitro root caries inhibited by phosphosilicate and fluoride dentifrices. Abstract 0501-UADR-2007.

Fejerskov O, Manji F (1990). Risk assessment in dental caries. In: Risk assessment in dentistry. Bader JD, editor. Chapel Hill: University of North Carolina Dental Ecology, pp. 215-217.

Fejerskov O, Thylstrup A (1994). Different concepts of dental caries and their implications. In: Textbook of clinical cariology. 2nd ed. Thylstrup A, Fejerskov O, editors. Copenhagen: Munksgaard, pp. 259-283.

Fejerskov O, Clarkson BH. Dynamics of caries lesion formation. In: Fejerskov O, Ekstrand J, Burt BA, editors. Fluoride in dentistry. 2nd ed. Copenhagen: Munksgaard; 1996; 187-214.

Gray GB, Shellis P: Infiltration of resin into white spot caries-like lesions of enamel: an in vitro study. Eur J Prosthodont Restor Dent 2002; 10: 27–32.

Harper DS, Osborn JC, Hefferren JJ, Clayton R. Cariostatic evaluation of cheeses with diverse physical and compositional characteristics. Caries Research 1986; 20: 123–30.

Hicks MJ, Flaitz C. Amorphous calcium phosphate-casein phosphopeptide paste: effect on enamel caries formation. JDR 2006; 85 (Special issue A) Abstract #0501.

Hojo K, Nagaoka S, Ohshima T, Maeda N. Bacterial interactions in dental biofilm development. J Dent Res. 2009 Nov; 88(11): 982-90. Review.

Hosoya N, Honda K, Lino F, Arai T. Changes in enamel surface roughness and adhesion of Streptococcus mutans to enamel after vital bleaching. Journal of Dentistry 2003; 31(8): 543-548.

Kielbasa AM, Paris S, Lussi A, etal. Evaluation of cavitations in proximal caries lesions at various magnification levels in vitro. J Dent 2006; 34(10): 817-822.

Kim HE, Kwon HK, Kim BI. Application of fluoride iontophoresis to improve remineralization. J Oral Rehab 2009; 36: 770-775.

Ko CC, Tantbirojn D, Wang T, Douglas WH. Optical scattering power for characterization of mineral loss. Journal of Dental Research 200; 79 (8): 1584-1589.

Krobicka A, Bowen WH, Pearson S, Young DA. The effects of cheese snacks on caries in desalivated rats. Journal of Dental Research 1987; 66: 1116–9.

Kugel G, Arsenault P, Papas A. Treatment modalities for caries management, including a new resin infiltration system. Compendium 2009; Oct 30 (Special Issue 3): 1-10.

LeGeros RZ. Calcium phosphates in enamel, dentin and bone. In: Myers HM, ed. Calcium phosphates in oral biology and medicine. Basel: Karger, 1991:108–129.

LeGeros RZ, Trautz OR, LeGeros JP, Klein E. Carbonate substitution in the apatite structure. Bull Soc Chim Fr 1968 (Spec Iss): 1712–1718.

LeGeros RZ. Calcium phosphates in oral biology and medicine. Basel: Karger, 1991.

Iijima Y, Cai F, Shen P, Walker G, Reynolds C, Reynolds EC. Acid resistance of enamel subsurface lesions remineralized by a sugar-free chewing gum containing casein phosphopeptides-amorphous calcium phosphate. Caries Res 2004; 38: 551-6.

Lopez L, Berkowitz R, Spiekerman C, Weinstein P. Topical antimicrobial therapy in the prevention of early childhood caries: a follow-up report. Pediatr Dent. 2002 May-Jun;24(3):204-6.

Lopez L, Stamford TC, Niederman R. Silver diamine fluoride: a caries "silver-fluoride bullet". J Dent Res. 2009 Feb;88(2):116-25.

Ly KA, Riedy CA, Milgrom P, Rothen M, Roberts MC, Zhou L. Xylitol gummy bear snacks: a school-based randomized clinical trial. BMC Oral Health. 2008 Jul 25;8:20.

Manji F, Fejerskov O, Nagelkerke NJD, Baelum V (1991). A random effects model for some epidemiological features of dental caries. Community Dent Oral Epidemiol 19: 324-328.

Margolis HC, Moreno EC. Composition and cariogenic potential of dental plaque fluid. Crit Rev Oral Biol Med. 1994; 5(1): 1-25. Review.

Martignon S, Ekstrand KR, Ellwood R. Efficacy of sealing proximal early active lesions: an 18 month clinical study evaluated by conventional and subtraction radiography. Caries Res 2006; 40: 382-8.

Matthijs S, Adriaens PA. Chlorhexidine varnishes: a review. J Clin Periodontol. 2002 Jan; 29(1): 1-8.

Meyer-Lueckel H, Paris S, Kielbassa AM. Surface layer erosion of natural caries lesions with phosphoric and hydrochloric acid gels in preparation for resin infiltration. Caries Res 2007; 41(3): 223-230.

Meyer-Lueckel H, Paris S: Progression of artificial enamel caries lesions after infiltration with experimental light-curing resins. Caries Res 2008; 42: 117–124.

Meyer-Lueckel H, Paris S, Mueller J, Cölfen H, Kielbassa AM. Influence of the application time on the penetration of different dental adhesives and a fissure sealant into artificial subsurface lesions in bovine enamel. Dent Mater 2006; 22: 22-8.

Milgrom P, Ly KA, Tut OK, Mancl L, Roberts MC, Briand K, Gancio MJ. Xylitol pediatric topical oral syrup to prevent dental caries: a double-blind randomized clinical trial of efficacy. Arch Pediatr Adolesc Med. 2009 Jul;163(7):601-7.

National Center for Health Statistics. Health, United States, 2010: With Special Feature on Death and Dying. Hyattsville, MD. 2011.

Nelson DGA, Featherstone JDB. Preparation, analysis, and characterization of carbonated apatites. Calcif Tissue Int 1982; 34: S69–S81.

Nelson DGA, Featherstone JDB, Duncan JF, Cutress TW. Effect of carbonate and fluoride on the dissolution behaviour of synthetic apatites. Caries Res 1983; 17: 200–211.

Nelson DGA, McLean JD. Direct observation of near-atomic details in synthetic and biological apatite crystallites. In: Fearnhead RW, Suga S, ed. Tooth Enamel IV. Amsterdam, Netherlands: Elsevier Science Publishers BV, 1984: 47–51.

Oikarinen KS, Nieminen TM. Influence of acid-etched splinting methods on di.scotoraxion of dental enamel in four media: an in vitro study. Scand J Dent Res 1994; 102: 313-318.

Paris S, Meyer-Luckel H, KielbassaAM. Resin Infiltration of natural caries lesion. J Dent Res 2007; 86: 662-6.

Paris S, Meyer-Lueckel H. Masking of labial enamel white spot lesions by resin infiltration-a clinical report. Quintessence International 2009; 40: 713-718.

Paris S,Dörfer CE, Meyer-Luckel H. Surface conditioning of natural enamel caries lesions in decidious teeth in penetration for resin infiltration. J Dent 2010; 38: 65-71.

Paris S, Meyer-Lueckel H, Mueller J, Hummel M, Kielbassa AM: Progression of sealed initial bovine enamel lesions under demineralizing conditions in vitro. Caries Res 2006; 40: 124–129.

Peters MC. Strategies for noninvasive demineralized tissue repair. Dental clinics of North America 2010; 54: 507-525.

Petersen PE, Bourgeois D, Ogawa H, Estupinan-Day S, Ndiaye C (2005). The global burden of oral diseases and risks to oral health. Bulletin of the World Health Organization, 83: 661-669.

Rao A, Malhotra N. The role of remineralizing agents in dentistry: A review. Compendium of Continuing Education in Dentistry; Jul/Aug 2011.

Reynolds EC, Cai F, Shen P, Walker GD. Retention in plaque and remineralization of enamel lesions by various forms of calcium in a mouthrinse or sugar-free chewing gum. J Dent Res 2003; 82: 206-11.

Reynolds EC. Anticariogenic complexes of amorphous calcium phosphate stabilized by casein phosphopeptides: a review. Spec Care in Dentist 1998; 18: 8-16.

Reynolds EC. Remineralization of enamel subsurface lesions by casein phosphopeptide-stabilized calcium phosphate solutions. JDR 1997; 76: 1587-95.

Reynolds EC, Johnson IH. Effect of milk on caries incidence and bacterial composition of dental plaque in the rat. Archives of Oral Biology 1981; 26: 445–51.

Reynolds RC. Casein phosphopeptide-amorphous calcium phosphate: the scientific evidence. Adv Dent Res 2009; 21: 25-29.

Reynolds EC, Cain CJ, Webber FL, et al. Anticariogenicity of calcium phosphate complexes of tryptic casein phosphopeptides in the rat. J Dent Res 1995; 74: 1272–1279.

Reynolds EC. The prevention of sub-surface demineralization of bovine enamel and change in plaque composition by casein in an intra-oral model. J Dent Res 1987; 66: 1120–1127.

Robinson C, Brookes SJ, Kirkham J, Wood SR, Shore RC. In vitro studies of the penetration of adhesive resins into artificial caries-like lesions. Caries Res 2001; 35: 136–141.

Rodda JC. Impregnation of caries-like lesions with dental resins. N Z Dent J. 1983; 79(358): 114-117.

Rosen S, Min DB, Harper DS, Harper WJ, Beck EX, Beck FM. Effect of cheese, with and without sucrose, on dental caries and recovery of Streptococcus mutans in rats. Journal of Dental Research 1984; 63: 894–6.

Schmidlin PR, Zehnder M, Pasqualetti T, Imfeld, T, Besek MJ: Penetration of a bonding agent into de- and remineralized enamel in vitro. J Adhes Dent 2004; 6: 111–115.

Stephan RM (1944). Intra-oral hydrogen-ion concentrations associated with dental caries activity. J Dent Res 23: 257-266.

Tant binjn D, Versluis A, Pintado MR, et al. Tooth deformation patterns in molars after composite restorations. Dent Mater 2004; 20(6): 535-542.

ten Cate JM, Featherstone JD. Mechanistic aspects of the interactions between fluoride and dental enamel. Crit Rev Oral Biol Med. 1991; 2(3): 283-96. Review.

ten Cate JM. Current concepts on the theories of the mechanism of action of fluoride. Acta Odont Scand 1999; 57: 325-9.

ten Cate JM. Remineralization of caries lesions extending into dentin. J Dent Res 2001; 80: 1407–1411.

ten Cate B. The role of saliva in mineral equilibria-caries, erosion and calculus formation. In: Edgar M, Dawes C, O'Mullane D, editors. Saliva and Oral Health. 3rd ed. London:BDJ Books; 2004: 120-35.

Torres Carlos Rocha Gomes, et al. Effect of caries infiltration technique and fluoride therapy on the colour masking of white spot lesions. Journal of Dentistry 2011; 39: 202-207.

White JM, Eakle WS. Rationale and treatment approach in minimally invasive dentistry. J Am Dent Assoc. 2000 Jun; 131 Suppl: 13S-19S. Review.

Wilson RA, Bullen HA. Basic Theory Atomic Force Microscopy Department of Chemistry, Northern Kentucky University 1986.

Wimpenny JWT (1994). The spatial organisation of biofilm. In: Bacterial biofilms and their control in medicine and industry. Wimpenny J, Nichols W, Stickler D, Lappin-Scott H, editors. Bioline, pp 1-5.

Yamamoto T, Ferracane JL, Sakaguchi RL, Swain MV. Calculation of contraction stresses in dental composites by analysis of crack propagation in the matrix surrounding a cavity. Dent Mater 2009; 15(3): 198-210.

Yee R, Holmgren C, Mulder J, Lama D, Walker D, van Palenstein Helderman W. Efficacy of silver diamine fluoride for arresting caries treatment. J Dent Res. 2009 Jul;88(7):644-7.